Constraints on Pacific Midplate Swells From Global Depth-Age and Heat Flow-Age Models

CAROL A. STEIN

Department of Geological Sciences, University of Illinois at Chicago, Chicago, IL 60680

SETH STEIN

Department of Geological Sciences, Northwestern University, Evanston, IL 60208

Oceanic midplate swells are identified by shallow seafloor depths. In turn, models of the processes giving rise to these regions rely on assessments of how their depths, surface heat flow, and flexural properties differ from those for lithosphere which is presumed not to have been affected by these processes. Such comparisons have been inhibited because reference thermal models, which are assumed to describe unperturbed lithosphere, predict deeper depths and lower heat flow than typically observed for lithosphere older than 70 Ma. As a result, both depth and heat flow anomalies can be overestimated. To address this difficulty, we have derived model GDH1 (Global Depth and Heat flow) by joint fitting of heat flow and bathymetry. GDH1, which has a hotter and thinner lithosphere than previous models, fits the depth and heat flow data significantly better, including the data from older lithosphere previously treated as anomalous. It also provides an improved fit to depth-to-basement data for ocean drilling sites, and to geoid offsets across fracture zones. The improved fit occurs for depth-age data from both the DBDB-5 digital bathymetry, and from regional medians from ship tracks, which yield comparable depth-age curves. We use GDH1 to study three classes of midplate swells: the Hawaiian and other hot spot swells, the Darwin Rise area of widespread Cretaceous volcanism, and the Superswell, considered a present analogue to the Darwin Rise. Heat flow on the Hawaiian swell, though anomalously high with respect to previous reference models, is at most slightly high relative to GDH1. The situation is similar for the Bermuda, Cape Verde, and Crozet hot spots. The absence of a significant heat flow anomaly favors a primarily dynamic, rather than thermal, origin for these swells. Similarly, the present depths and heat flow for the Darwin Rise are consistent with GDH1, although they were anomalous with respect to previous reference models. The depth and heat flow data thus provide no evidence for the Darwin Rise being thermally different at present from lithosphere of the same age elsewhere. The situation for the Superswell is similar to that for Hawaii, in that the heat flow data are consistent with those for unperturbed lithosphere, despite the shallow bathymetry. Flexural data for the Superswell indicate that the lithosphere was anomalously weak at the time of seamount loading. This also appears to have been the case for the Darwin Rise, but not for the Hawaiian or other swells. Although the weakness has been interpreted as due to elevated temperatures in the lithosphere, the required high temperatures should give rise to heat flow much higher than observed. Hence the flexural strength anomaly with respect to Hawaii and other swells suggests that the lithosphere for the Superswell and Darwin Rise has been mechanically weakened by the cumulative action of multiple hot spots.

Attention is once again focusing on the timing and mechanisms of midplate volcanism as a major factor in the vertical tectonic history of the Central Pacific.

Schlanger and Premoli-Silva, 1981

The Mesozoic Pacific: Geology, Tectonics, and Volcanism
Geophysical Monograph 77

INTRODUCTION

Understanding the nature and origin of significant vertical crustal motion in the Pacific Basin has been a challenge since its identification by Darwin [1845]. Menard [1964] proposed that a large region of shallow bathymetry in the Western Pacific, which he termed the Darwin Rise, had undergone major volcanism and uplift during the Cretaceous (Figure 1). This region (Figure 2) includes the Mid-Pacific Mountains, the Marshall Islands, the Magellan Seamounts, and the Wake Guyots. With the advent of plate tectonics, it became clear that the formation

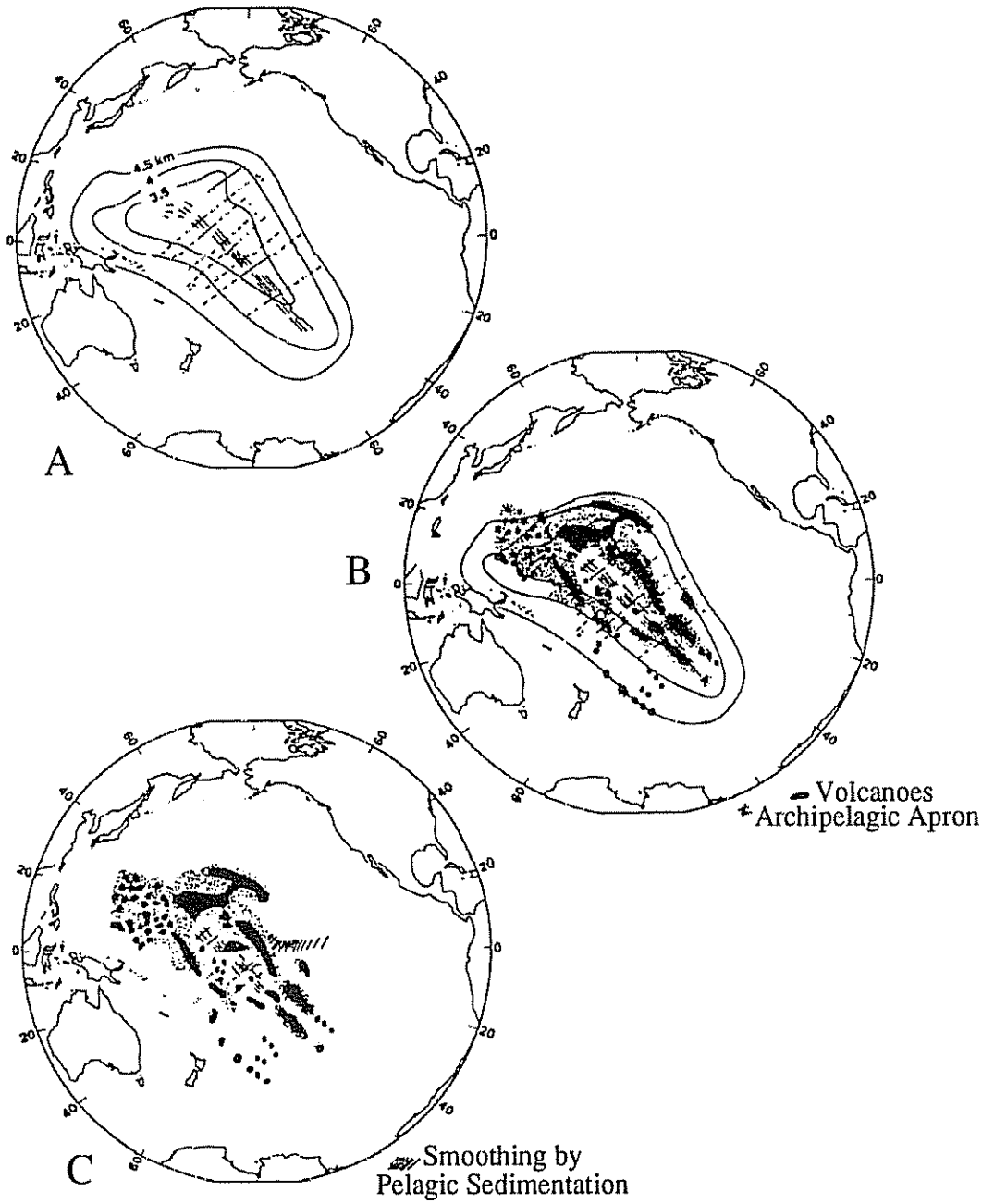

Fig. 1. Menard's [1964] model for the evolution of the Darwin Rise by elevation of a broad region (A), widespread Late Mesozoic volcanism (B), and Cenozoic subsidence (C).

of the Darwin Rise was a striking example of midplate volcanism. Subsequently, considerable effort has been devoted to investigating the processes responsible for the Darwin Rise and other midplate volcanism and uplifts.

At present, the origin of the Darwin Rise is generally thought to be related to the effects of mantle plumes [Morgan, 1972]. Crough [1979] noted that the present Easter and Macdonald hot spots would have been under the Darwin Rise during the period of uplift and volcanism, and proposed that the region represented a series of seamounts formed along these tracks, rather a broad area simultaneously uplifted. By analogy to the present Hawaiian hot spot, Crough proposed that the hot spots were also associated with broad swells [Crough, 1978; Detrick and Crough, 1978] which gave rise to regional uplifts. Deep sea drilling, however, provided evidence for widespread volcanism in the area in addition to the seamounts, leading to the

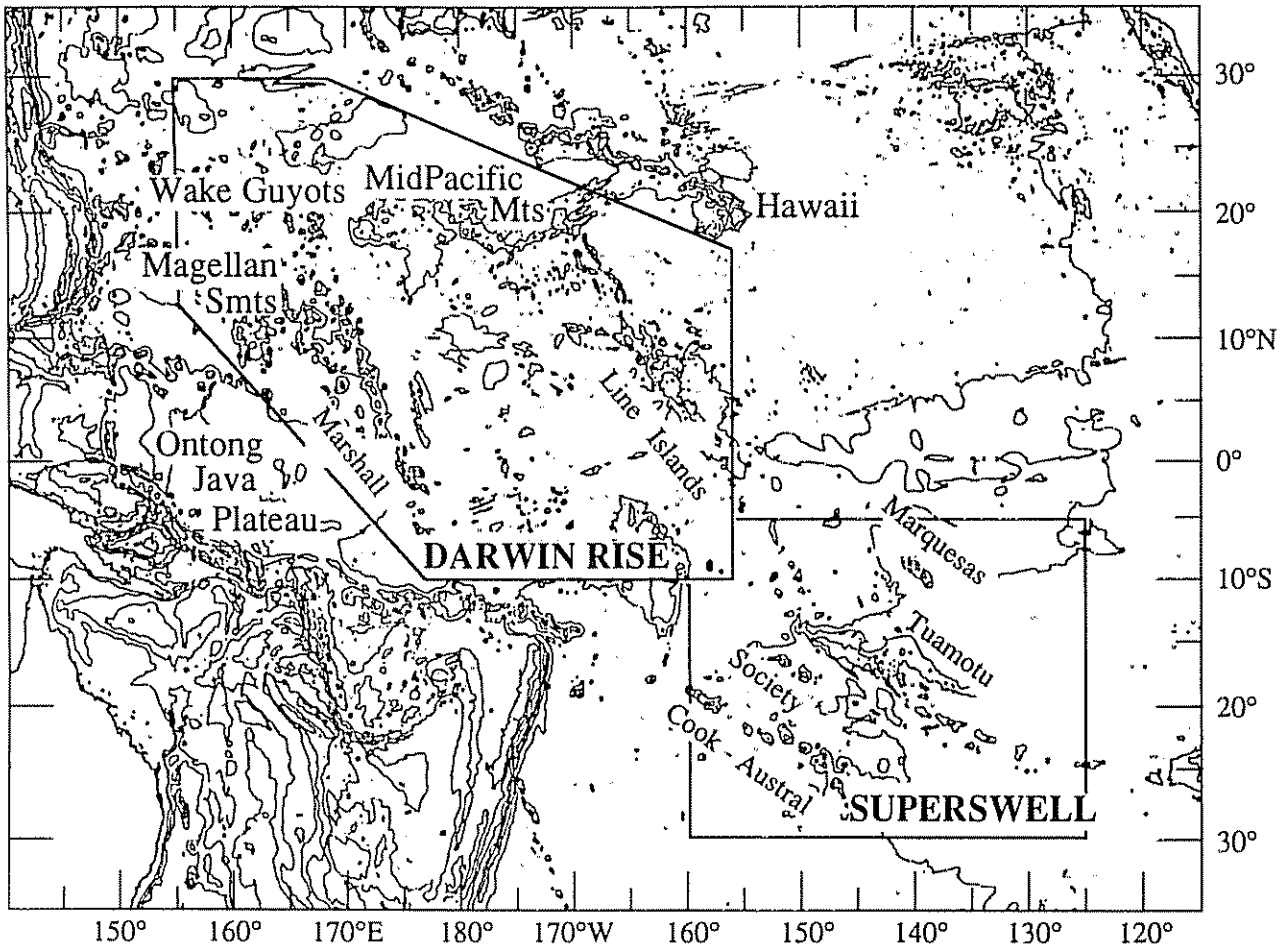

Fig. 2. Bathymetry of the Pacific, showing the regions we used for Darwin Rise and Superwell depth and heat flow analyses. Because the extent of the Superwell and Darwin Rise are ill-defined, the boundaries of the regions we used are somewhat arbitrary.

suggestion that the areal extent and magnitude of the volcanism and uplift exceeded that which might be expected from multiple hot spot tracks [Winterer, 1973; 1976; Jackson and Schlanger, 1976; Schlanger and Premoli-Silva, 1981; Larson and Schlanger, 1981; Schlanger et al., 1981]. Menard [1984] therefore proposed that the hot spot model could be reconciled with the regional uplift and volcanism by assuming that the Cretaceous Darwin Rise was similar to the present area extending from the East Pacific Rise to the Society Islands. He considered this area, termed the Polynesian Plume Province (PPP) [Vogt, 1981], to contain both a broad regional uplift and a number of hot spot swells, including the Cook-Austral, Marquesas, Pitcairn, and Society seamount chains. These hot spot tracks have formed volcanic edifices in the past 18 Ma [Duncan and Clague, 1985], giving rise to a complex pattern of volcanic ages and types. Holocene volcanism occurs at several sites on the chains, and the NW-SE trend of the plateaus and island chains is similar to that of the Hawaiian hot spot track. Because many of these hot spot tracks can be traced back to the Darwin Rise, a similar situation might have formed the Darwin Rise.

McNutt and Fisher [1987] proposed the term "Superswell" for the PPP, and further developed the concept of this area as a present-day analog to the Darwin Rise. They noted that the Superswell area, from west of the East Pacific Rise to approximately 160°W, 9-30°S is substantially shallower than expected for its age, which ranges from 20 to 90 Ma. In addition, the effective elastic thicknesses of the lithosphere calculated from the loading of volcanoes and seamounts are substantially less than expected for the age of loading [McNutt and Menard, 1978; Calmant and Cazenave, 1987; Calmant et al., 1990]. McNutt and Fisher suggested that the shallow bathymetry resulted from the lithosphere in the area having the temperature structure of an anomalously thin 75-km thick thermal plate. McNutt and Judge [1990] further suggested that the weak flexural strengths, low surface wave velocities [Nishimura and Forsyth, 1985], and geochemical anomalies [Hart, 1984, 1988;

Castillo, 1988] were consequences of the combined effects of a thin thermal plate and a deeper low-density plume. In this model, the lithosphere is thinned by enhanced heat flux from the mantle and low viscosity beneath the plate, such that the weak plate is easily penetrated by hot spot volcanism. The net volume flux of the Superswell plume has been estimated as approximately 30% of the total global plume flux, a flux exceeding that of the Hawaiian plume, thought to be the single largest [Sleep, 1990].

Extending this analysis, McNutt and Fisher [1987] interpreted the Darwin Rise as also anomalously shallow for its age. They noted other similarities to the Superswell, including similar petrologic anomalies [Hart, 1984; Natland and Wright, 1984]. In addition, the effective elastic thicknesses are lower than expected for the age of loading [Calmant, 1987; Calmant and Cazenave, 1987; Smith et al., 1989; Wolfe and McNutt, 1991]. McNutt et al. [1990] suggested a schematic history in which the Darwin Rise was dynamically uplifted during the Cretaceous, and was then similar to the present Superswell until about 70–80 Ma. The present depth was thus interpreted as anomalously shallow, indicating a residual effect of the transient Cretaceous reheating. Larson [1991] termed the Cretaceous event a "Superplume," which produced both the Darwin Rise and very large amounts of lithosphere at midocean ridges. In this model, the present Superswell reflects the Superplume's waning phase. Davies and Pribac [this volume] propose that the Darwin Rise and Superswell reflect the effect of both plume material and anomalously warm deep mantle material.

Models for the Darwin Rise and Superswell thus combine aspects of the two basic models that have been proposed for the origin of hot spot swells. In one model, the swell is a thermal effect due to the hot spot thinning and heating the lithosphere at depth [Detrick and Crough, 1978; Von Herzen et al., 1982]. In the second model, the uplift is primarily due to the dynamic effects of the upwelling plume [Parsons and Daly, 1983; Courtney and White, 1986; Robinson and Parsons, 1988; Sleep, 1992], which may largely reflect thermal buoyancy forces within the upwelling mantle [Liu and Chase, 1989; 1991]. Thus the Darwin Rise and Superswell may reflect, at least in part, perturbations to the thermal structure of the lithosphere, as evidenced by depth and flexural strength anomalies relative to unperturbed lithosphere of the same age. Similarly, the possible thermal perturbations associated with smaller "ordinary" swells are modeled using as constraints depth, heat flow, and flexural strength anomalies. As a result, tectonic interpretations can depend significantly on the reference model which is assumed to characterize the thermal evolution of unperturbed ("normal") lithosphere, and its corresponding predictions for the variation in depth and heat flow as functions of age. In this paper, we discuss the selection of a reference model, and explore its implications for tectonic interpretations of hot spot swell regions.

REFERENCE MODEL GDH1

Motivation

Studies of lithospheric processes, such as the origin of the Darwin Rise and Superswell, make use of a reference model in two complementary ways. First, the predicted variations in depth and heat flow as functions of age are used to identify and characterize anomalous regions. Second, the thermal structure model is assumed to characterize unperturbed lithosphere, and thus provide a basis by which the inferred depth and heat flow perturbations are used to estimate thermal perturbations and corresponding perturbations in temperature-dependent physical properties such as material strength or seismic velocity.

Reference models are developed using as constraints the decrease in heat flow and increase in seafloor depth with age as lithosphere formed at high temperature cools as it spreads away from the ridge (Figure 3). These data jointly reflect the evolution with age of the lithospheric geotherm, because the bathymetry depends on the temperature integrated over depth and the heat flow depends on the temperature gradient at the sea floor.

The simplest reference model is one in which the lithosphere behaves as the cold upper boundary layer of a cooling halfspace, such that depth and heat flow vary as age$^{1/2}$ and

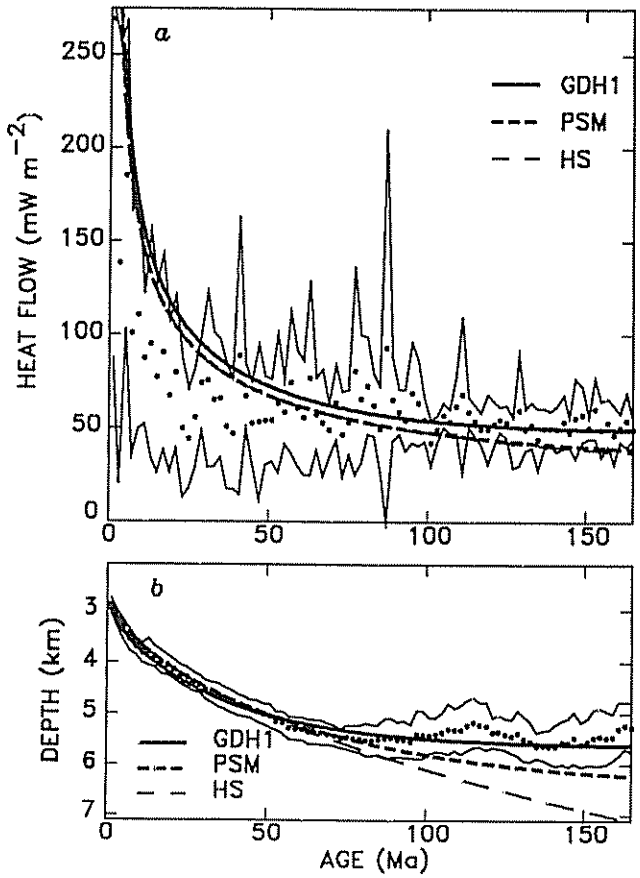

Fig. 3. Data and models for heat flow and ocean depth as a function of age. Data are averaged in two-m.y. bins, and one standard deviation about the mean value for each is shown by the envelope. Also shown are the predicted values for the plate model of Parsons and Sclater [1977] (PSM), a cooling halfspace model with the same thermal parameters (HS), and the GDH1 plate model. Heat flow for the HS and PSM curves overlap for ages younger than ~120 Ma. [Stein and Stein, 1992].

age$^{-1/2}$, respectively [Davis and Lister, 1974]. This model, with reasonable values for the physical parameters, describes the primary features of the depth and heat flow variations. Subsequently, however, it was recognized that the depth and heat flow data "flatten", varying more slowly with age for older lithosphere (Figure 3). Most recent studies thus use a reference model in which the lithosphere is treated as a cooling plate with an isothermal lower boundary [Langseth et al., 1966; McKenzie, 1967; Parsons and Sclater, 1977]. For young ages, the plate behaves like a cooling halfspace, but for older ages, the effects of the lower boundary cause the depth and heat flow curves to flatten.

The lower isothermal boundary condition models the additional heat input from below, which is assumed to prevent the halfspace from continuing to cool for older ages. Various mechanisms including radiogenic heat [Crough, 1977], shear heating [Schubert et al., 1976], small-scale convection [Parsons and McKenzie, 1978; Parsons and Richter, 1981], and mantle plumes [Heestand and Crough, 1981] have been proposed as sources of this additional heat. In most of these formulations, the asymptotic plate thickness to which the lithosphere evolves corresponds to the depth at which the additional heat is supplied, and above which temperature changes cause bathymetric variations. Because the thermal structure within the lithosphere does not depend critically on how this heat is supplied [Parsons and McKenzie, 1978], the plate model has become a standard for comparing the predicted temperatures within the lithosphere to other data including seismic surface wave velocities [Forsyth, 1977; Sato et al., 1989], flexure due to applied loads [Bodine et al., 1981] and the depths of intraplate earthquakes [Wiens and Stein, 1983; Chen and Molnar, 1983].

Parsons and Sclater [1977] found that such a model, with a 125 km thick plate with 1350°C basal temperature, provided good fits to the data then available. It described the general shape of the depth curve, including the flattening for ages > 70 Ma, and the heat flow for ages > 50 Ma. Its major limitation, the underprediction of heat flow for ages < 50 Ma, is thought to result from the transport of significant amounts of heat by water circulation [Lister, 1972; Anderson and Hobart, 1976; Wolery and Sleep, 1976]. The Parsons and Sclater model (a term often applied to a plate model with the parameters they estimated from the available data), has become a standard model for the lithosphere.

For studies of processes that may have formed hot spot swells, however, the Parsons and Sclater model (hereafter, PSM) has serious limitations. It predicts deeper depths and lower heat flow than generally observed for lithosphere older than 70-100 Ma (Figure 3). As a result, depth data [Kaula and Philips, 1981; Sclater and Wixon, 1986; Renkin and Sclater, 1988; Marty and Cazenave, 1989; Colin and Fleitout, 1990; Smith, 1990; Stein and Abbott, 1991] and heat flow data [Detrick et al., 1986; Louden et al., 1987; Von Herzen et al., 1989; Lister et al., 1990; Langseth et al., 1990; Stein and Abbott, 1991] for older lithosphere typically appear anomalous. Hence an area with depth or heat flow anomalous with respect to PSM need not differ from the average lithosphere of that age.

Derivation

To alleviate this difficulty, we have developed a new reference model by a combined analysis of recent depth and heat flow data [Stein and Stein, 1992]. We used a global heat flow data set derived primarily from a published compilation [Louden, 1989], with additional data some of which have been reported elsewhere [Stein and Abbott, 1991]. Because the heat flow and depth for old lithosphere are crucial joint constraints, the model was derived with only data from regions where the published depth data extend to at least 166 Ma and have been corrected for sediment thicknesses. The combined depth data for these areas, the Northwestern Atlantic [Sclater and Wixon, 1986] and North Pacific [Renkin and Sclater, 1988], and the corresponding heat flow data are shown in Figure 3, and listed in Table 1.

We used the depth data for all ages and the heat flow data for ages greater than 50 Ma to constrain the primary parameters of a plate model: lithospheric thickness (a), basal temperature (T_m), and coefficient of thermal expansion (α). Figure 4a-c shows contours of the misfit to the data as a function of basal temperature and thickness, for the best fitting coefficient of thermal expansion, 3.1×10^{-5} °C^{-1}. These plots show a slice of the three dimensional model space with the coefficient of thermal expansion fixed. Figure 4d shows the misfit as a function of the coefficient of thermal expansion and basal temperature, for the best fitting thickness of 95 km, and Figure 4e shows the misfit as a function of the coefficient of thermal expansion and thickness, for the best fitting basal temperature, 1450°C.

The misfit contours for the depth data show a diagonal pattern, because the asymptotic depth for infinitely old age is proportional to the product of plate thickness and basal temperature. The best fit is for a thinner plate and somewhat higher basal temperature than in PSM, consistent with the observed depths (Figure 3) being shallower than predicted by PSM. The heat flow data for lithosphere older than 50 Ma provide a separate constraint. The misfit contours are elongated in the opposite sense as for the depths, because the asymptotic heat flow for infinitely old age depends on the ratio of basal temperature to thickness. As for the depths, the best fit occurs for a thinner plate and hence higher T_m/a than for PSM, because the observed heat flow exceeds that predicted by PSM. The coefficient of thermal expansion plots show the best fitting value, and the partial tradeoffs due to the fact that the depths for young and old ages depend on the products αT_m and $\alpha T_m a$, respectively. Joint fitting of the combined depth and heat flow data gives a best fit for a 95 km thick plate, with a basal temperature of 1450°C, and a coefficient of thermal expansion of 3.1×10^{-5} °C^{-1}. The model parameters are listed in Table 2.

The depth and heat flow predictions for this model, which we call GDH1 (for Global Depth and Heat flow), are accurately approximated using a halfspace model with the same parameters for young lithosphere, and the first term of the series solution for old lithosphere [Stein and Stein, 1992]. The depth (m) is related to the age (Ma) by

$$d(t) = 2600 + 365\, t^{1/2} \qquad t<20 \text{ Ma}$$

$$= 5651 - 2473 \exp(-0.0278\, t) \qquad t\geq20 \text{ Ma}$$

TABLE 1: Data for GDH1 Model

Age range (Ma)	Depth (m)	Heat flow (mW m^{-2})	Age range (Ma)	Depth (m)	Heat flow (mW m^{-2})
0 - 2	2896 ± 139	269 ± 182	82 - 84	5519 ± 304	62 ± 17
2 - 4	3176 ± 162	138 ± 118	84 - 86	5516 ± 298	50 ± 23
4 - 6	3378 ± 196	185 ± 82	86 - 88	5482 ± 380	93 ± 117
6 - 8	3568 ± 208	101 ± 66	88 - 90	5477 ± 385	65 ± 22
8 - 10	3700 ± 162	110 ± 61	90 - 92	5514 ± 338	59 ± 12
10 - 12	3832 ± 187	87 ± 35	92 - 94	5507 ± 363	54 ± 16
12 - 14	3811 ± 264	95 ± 61	94 - 96	5542 ± 321	69 ± 27
14 - 16	3898 ± 207	77 ± 51	96 - 98	5415 ± 476	63 ± 23
16 - 18	4001 ± 227	90 ± 52	98 - 100	5417 ± 460	55 ± 12
18 - 20	4065 ± 198	67 ± 41	100 - 102	5435 ± 357	42 ± 12
20 - 22	4142 ± 189	79 ± 41	102 - 104	5416 ± 333	49 ± 7
22 - 24	4244 ± 194	50 ± 37	104 - 106	5377 ± 389	57 ± 7
24 - 26	4303 ± 197	44 ± 26	106 - 108	5305 ± 496	54 ± 7
26 - 28	4388 ± 188	56 ± 27	108 - 110	5319 ± 410	62 ± 15
28 - 30	4430 ± 173	74 ± 26	110 - 112	5320 ± 479	68 ± 42
30 - 32	4547 ± 183	75 ± 47	112 - 114	5232 ± 488	59 ± 8
32 - 34	4605 ± 203	65 ± 36	114 - 116	5177 ± 487	54 ± 8
34 - 36	4652 ± 226	66 ± 32	116 - 118	5213 ± 440	50 ± 9
36 - 38	4715 ± 217	51 ± 33	118 - 120	5249 ± 466	50 ± 19
38 - 40	4769 ± 224	47 ± 29	120 - 122	5372 ± 294	53 ± 12
40 - 42	4836 ± 209	89 ± 75	122 - 124	5355 ± 330	55 ± 7
42 - 44	4871 ± 193	67 ± 18	124 - 126	5402 ± 310	53 ± 9
44 - 46	4915 ± 175	53 ± 22	126 - 128	5446 ± 331	42 ± 14
46 - 48	4967 ± 208	53 ± 41	128 - 130	5388 ± 444	60 ± 30
48 - 50	5015 ± 198	54 ± 24	130 - 132	5495 ± 436	49 ± 11
50 - 52	5056 ± 225	54 ± 22	132 - 134	5545 ± 394	52 ± 12
52 - 54	5151 ± 187	63 ± 37	134 - 136	5628 ± 252	44 ± 16
54 - 56	5181 ± 212	58 ± 17	136 - 138	5625 ± 296	50 ± 11
56 - 58	5287 ± 224	74 ± 38	138 - 140	5639 ± 319	50 ± 9
58 - 60	5306 ± 221	61 ± 31	140 - 142	5628 ± 405	50 ± 12
60 - 62	5303 ± 217	55 ± 30	142 - 144	5558 ± 427	54 ± 14
62 - 64	5358 ± 237	77 ± 52	144 - 146	5567 ± 472	48 ± 8
64 - 66	5367 ± 233	57 ± 20	146 - 148	5470 ± 505	55 ± 21
66 - 68	5374 ± 236	53 ± 29	148 - 150	5602 ± 437	57 ± 15
68 - 70	5400 ± 210	49 ± 15	150 - 152	5555 ± 455	50 ± 6
70 - 72	5436 ± 204	64 ± 20	152 - 154	5474 ± 541	60 ± 16
72 - 74	5489 ± 185	47 ± 23	154 - 156	5449 ± 565	49 ± 15
74 - 76	5466 ± 236	53 ± 17	156 - 158	5476 ± 518	53 ± 13
76 - 78	5484 ± 252	81 ± 56	158 - 160	5456 ± 450	46 ± 16
78 - 80	5496 ± 262	66 ± 34	160 - 162	5299 ± 533	50 ± 8
80 - 82	5519 ± 322	72 ± 26	162 - 164	5229 ± 465	54 ± 14
			164 - 166	5270 ± 489	49 ± 5

and the heat flow (mW m^{-2}) is

$$q(t) = 510\, t^{-1/2} \qquad t \leq 55 \text{ Ma}$$

$$= 48 + 96 \exp(-0.0278\, t) \qquad t > 55 \text{ Ma}.$$

(The t^2 term in the expression for young depths in Stein and Stein [1992] is a typographical error.)

GDH1 fits the data significantly better than PSM, especially for old lithosphere (Figure 3). For the dataset we use, the mean and standard deviation of the depth and heat flow for lithosphere older than 140 Ma are 5464 ± 484 m and 52 ± 13 mW m^{-2}. GDH1 predicts an asymptotic depth for infinitely old lithosphere of 5651 m, considerably shallower than the 6400 m for PSM. The asymptotic heat flow for GDH1 is 48 mW m^{-2}, approximately 40% higher than the 34 mW m^{-2} value for PSM. An F-ratio test indicates that the improved fit to the depth and heat flow data is significant above the 99.9% level. Figure 4f shows that the improved fit of GDH1 relative to PSM is comparable to

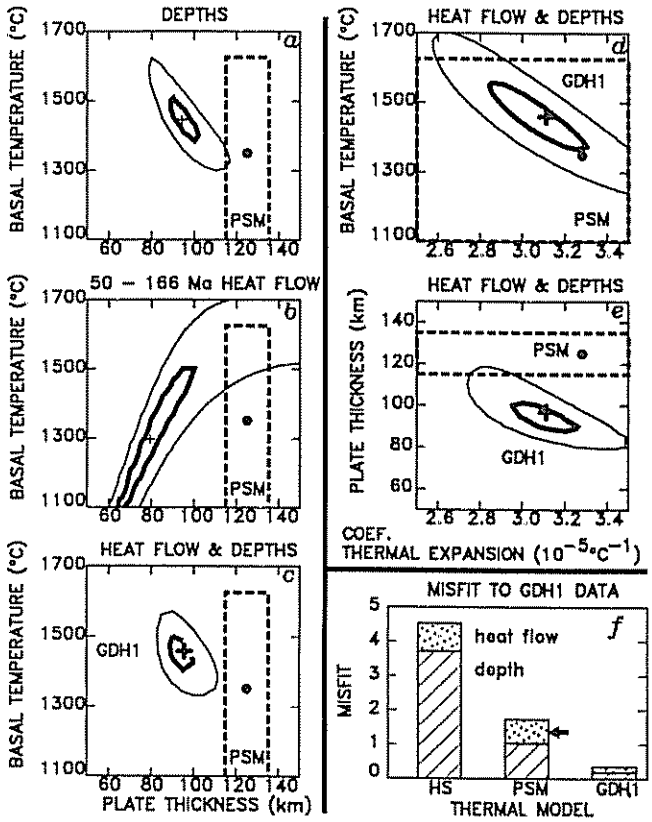

Fig. 4. (a-e): Contour plots of the misfit to subsets of the data as a function of combinations of the three parameters. In each panel, the best fit is denoted by a cross, and the contours show values 1.25 and 2.5 times the minimum misfit. Parsons and Sclater's values (PSM) and their estimated uncertainties are also indicated. The best fitting solution for the combined depth and heat flow (c-e), a 95 km thick plate with a basal temperature of 1450°C and coefficient of thermal expansion, 3.1×10^{-5} °C^{-1} is model GDH1. (f): Misfit to the data for GDH1, PSM, the halfspace model, and a version of the PSM model including radioactivity (arrow), which predicts the same depths but higher heat flow than PSM. [Stein and Stein, 1992].

that for PSM relative to the halfspace model. An F-ratio test shows that GDH1 also provides an improved fit above the 99.9% level relative to a version of the PSM model in which in addition to the heat flow due to plate cooling, 4 mW m^{-2} is assumed to be generated by radioactivity [Parsons and Sclater, 1977], giving the same depths as PSM but a better fit to the heat flow.

GDH1 was developed by joint fitting of heat flow and bathymetry. The heat flow data alone [Stein and Stein, 1992] are best fit by a model with an 80 km thick lithosphere and a 1300°C basal temperature, corresponding to a 6% higher (51 mW m^{-2}) asymptotic heat flow than for GDH1. Such a heat flow-only model is poorly constrained due to the lack of depth data. It illustrates, however, that GDH1 slightly underpredicts the heat flow data.

TABLE 2: GDH1 model parameters

a	plate thickness	95 km
T_m	basal temperature	1450 °C
α	thermal expansion coefficient	3.1×10^{-5} °C^{-1}
k	thermal conductivity	3.138 W m^{-1} °C^{-1}
C_p	specific heat	1.171 kJ kg^{-1} °C^{-1}
ρ_m	mantle density	3330 kg m^{-3}
ρ_w	water density	1000 kg m^{-3}
d_r	ridge depth	2600 m

GDH1 is representative of the plate models that fit the data well. Quantification of the true uncertainties in model parameters is difficult, given the limitations of the data and model. From examination of fits to the data, we estimate the plate thickness as 95 ± 15 km, basal temperature as 1450 ± 250°C, and α as $3.1 \pm 0.8 \times10^{-5}$ °C^{-1}, where the uncertainties are one standard deviation, and do not include the uncertainty in the model or other parameters (e.g. conductivity). Alternatively, if we regard α as known a priori, we estimate the thickness and T_m uncertainties as 10 km and 100°C, respectively. Thus our solutions have plate thicknesses generally less than Parsons and Sclater's estimate (125 ± 10 km), basal temperatures comparable to their estimate (1350 ± 275°C), and α comparable to their estimate ($3.2 \pm 1.1 \times10^{-5}$ °C^{-1}).

Properties Of Reference Models

Thermal models of the lithosphere are used in several ways for tectonic studies. First, they provide reference models to characterize the average variation in depth and heat flow with age for assumed-"normal" lithosphere. It is thus possible to identify regions which are anomalous with respect to a reference model, and to estimate how anomalous the depth and heat flow are. Second, a model predicts a temperature structure for "normal" lithosphere, and hence can be used to draw inferences about the processes giving rise to the temperature structure of both "normal" and "anomalous" lithosphere. These two applications are somewhat decoupled, in that it is useful to characterize "normal" lithosphere and identify anomalies, although the assumed thermal structure presumably approximates a more complex situation.

The reference model is thus used to distinguish "normal" lithosphere, that characterized by normal heat flow and depth, from "anomalous" lithosphere. Moreover, lithosphere can be characterized as either thermally anomalous, in that both its depth and heat flow are anomalous, presumably due to elevated temperatures in the lithosphere, or topographically anomalous, presumably due primarily to mantle flow. Table 3 summarizes these end member cases. As discussed shortly, hot spot swells appear to be closer to topographic anomalies than thermal ones.

This classification relies on the fact that we, like Parsons and Sclater [1977], find a consistent thermal model by fitting the depth and heat flow jointly. Although empirical curves could be derived for either data type alone, they are generally less useful in investigating thermal structure. First, there is no requirement that the other data type be well fit. Second, an empirical depth-

TABLE 3: End Member Lithospheric Types

Normal Lithosphere	Topographically Anomalous Lithosphere	Thermally Anomalous Lithosphere
Heat flow and depth fit reasonably well by GDH1	Depth significantly shallow with respect to GDH1: Heat flow normal or slightly elevated	Depth significantly shallow and heat flow significantly high with respect to GDH1
Most >70 Ma lithosphere; Darwin Rise (at present)	Hotspot swells (Hawaii, Bermuda, Cape Verde, Crozet) and Superswell	?
Normal lithospheric thermal structure	Primarily dynamic uplift	Anomalous lithospheric thermal structure

age curve often achieves a better fit to data because it treats the young and old depths separately [Smith, 1990] and hence contains a greater number of parameters than a plate model. The improved fit is thus meaningful only if it exceeds that expected purely by chance due to the additional free parameters. Third, because constants in such models which correspond to combinations of the thermal model parameters are estimated independently, they can yield inconsistent values of the thermal model parameters, and thus be of little value in predicting the geotherm. In contrast, joint fitting of depth and heat flow assumes that both variations reflect the cooling of the lithosphere.

GDH1, like most thermal models for the lithosphere, is phenomenological in that it was derived to be the simplest model that describes the observed variation in depth and heat flow. These variations may in part also reflect other possible effects, some of potential significance, which are not included in the model [Stein and Stein, 1992]. Of special importance for our discussion here is that the variation in depth with age is assumed to result entirely from the temperature structure of the lithosphere [Parsons and McKenzie, 1978], whereas depth effects can also reflect sublithospheric processes [Hager and O'Connell, 1980; Buck and Parmentier, 1986; Davies, 1988; Jarvis and Peltier, 1989; Davies and Pribac, this volume]. In addition, the plate model used here does not incorporate time dependent effects beyond cooling, such as might be associated with the proposed Cretaceous superplume [Larson, 1991]. Determination of the magnitude of these possible effects not included in the plate model has long been challenging precisely because the simple plate model fits the two primary surface observables, depth and heat flow, reasonably well. Although the depth-age and heat flow-age curves are derived assuming a thermal model, their utility is not directly tied to the appropriateness of the thermal model.

The choice of the data used to derive the model is crucial. Some data must be excluded because of biases, but as more data are excluded, the resulting model is increasingly influenced by a priori assumptions about the processes being described. For example, we have chosen not to fit the heat flow data in young lithosphere, because of the assumed bias from hydrothermal flow. We have not attempted to remove the effect of hot spot swells, because removing swells requires using an a priori reference model to decide which lithosphere is anomalously shallow, which in turn influences the resulting view of what depths are "normal." Our approach differs from Parsons and Sclater's largely in the choice of which depths for old lithosphere to fit. Their approach, fitting a model to the deepest old lithosphere, caused the remaining old lithosphere to appear shallow. We instead fit a model to all the depth data. By doing so, we assume that whether the temperature structure causing flattening of the depth curve reflects small scale convection, hot spot reheating, or other processes, an appropriate global reference model should reflect their average effects.

An alternative view is to adopt the cooling halfspace model as the reference [Davies and Pribac, this volume]. With this reference almost all old lithosphere is anomalous, and the degree to which it is anomalous indicates the perturbation to the cooling halfspace. Thus lithosphere which would be called "normal" relative to GDH1 would be perturbed by the "usual" amount for its age relative to a halfspace. A disadvantage with the halfspace reference model is that it is harder to identify regions of old lithosphere which are significantly more perturbed than most old lithosphere.

Implicit in our approach, in which the model is fit to the data, is that the model depends on the data used to derive it. In particular, given that old lithosphere is restricted to a few regions, the choice of data has an important effect. Successive reference models are improvements over previous models, in that they better fit more of the data that the previous ones could not. Nonetheless, the differences in subsidence rates between plates and within plates are substantial enough [Davis and Lister, 1974; Cochran, 1986; Hayes, 1988; Marty and Cazenave, 1989] that no single model can perfectly represent the data. Similarly, our fitting of mean depths, which are convenient for statistical analysis, or the alternative of fitting modal depths,

which are less affected by processes which produce shallow depths, affects the result somewhat, as discussed shortly. As a result, any global reference model is an approximation to an unattainable ideal.

TESTS OF THE GDH1 MODEL

Before applying the GDH1 model to study midplate swells, we examined how well the model fit several other data sets.

Drill Site Data

First, we considered a global data set of the basement depths (corrected for sediment) versus age compiled for all DSDP and ODP drill sites which recovered normal tholeiitic extrusive basalts [Johnson and Carlson, 1992]. This test has several advantages. First, these data were not used in deriving GDH1. Second, the basement depths and ages are well constrained for the drill site data. Third, these data include sites in the Indian Ocean, whereas no Indian Ocean data were used to derive GDH1. Figure 5 shows that GDH1 offers a significantly better fit than PSM (a 56% misfit reduction). An independent analysis of these depth data [Johnson and Carlson, 1992] yielded a best-fitting plate model with a thicknesses of 105 ± 10 km and a basal temperature of 1400 ± 140°C, values quite consistent with GDH1.

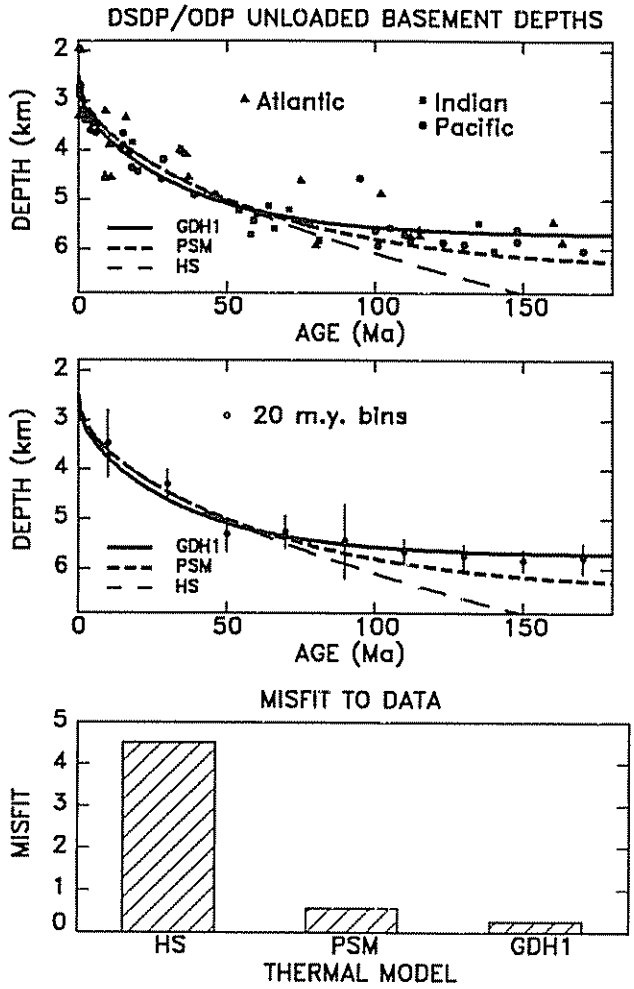

Fig. 5. Top: Fits to a global data set of the basement depths (corrected for sediment) versus age for DSDP and ODP drill sites [Johnson and Carlson, 1992]. The curves are for GDH1, the plate model of Parsons and Sclater [1977] (PSM), and a cooling halfspace model with the same thermal parameters (HS). These data were not used to derive GDH1. Center: Fits to this data set combined into 20 My bins. Bottom: Net misfit to the binned data. GDH1 offers a significantly better fit than PSM (a 56% misfit reduction).

Ocean-specific Data

Next, we tested the possibility that GDH1's good fits to the old lithosphere in the Pacific, which are especially important in this paper, might merely reflect the use of these depths in deriving it. To address this issue, we found best fitting plate model parameters separately for the North Pacific and Northwest Atlantic data, using the same procedure as for GDH1. The resulting models, NPC1 and NWA1, both have 90 km thick plates with a basal temperature of 1375°C. The coefficients of thermal expansion differ, being 3.3×10^{-5} °C^{-1} and 3.5×10^{-5} °C^{-1}, respectively. Alternatively, if we require that the coefficient of thermal expansion be that used in the GDH1 model, 3.1×10^{-5} °C^{-1}, we find models NPC2, a 95 km thick plate with a 1425°C basal temperature, and NWA2, a 95 km thick plate with a 1400°C basal temperature. For convenience, we refer to these models by name, with those ending in "2" being those derived with a fixed coefficient of thermal expansion. Chosing between the two members of the pairs of models is largely a matter of taste; keeping the coefficient of thermal expansion the same is attractive philosophically, but the improved fits resulting from allowing the additional free parameter are statistically significant as measured by an F-ratio test. As discussed later, the apparent variation in the coefficient of thermal expansion probably reflects limitations of the simple plate model.

Comparison of ocean-specific models NPC1 and NWA1 to the data (Figure 6) illustrates both similarities and differences. The average heat flow as a function of age is similar for the two plates, although as previously noted the Atlantic data have larger scatter to older ages [Anderson and Skilbeck, 1981]. The predicted heat flow, which does not depend on the coefficient of thermal expansion, is the same for these two models. The depths, however, are different between the two oceans. For ages less than about 70 Ma, the depths are similar. For older ages, however, the Pacific is generally shallower. For the dataset we use (Table 1), the mean depth and standard deviation for ages older than 100 Ma is 5423 ± 432 m, an average of the Atlantic and Pacific values of 5649 ± 308 and 5197 ± 807 m, respectively. NWA1, with a larger coefficient of thermal expansion, fits the deeper Atlantic depths for old lithosphere reasonably well. NPC1, however, does not fit the shallower Pacific depths for old lithosphere as well. The misfit presumably reflects the fact that much of the shallow topography in the Pacific, such as

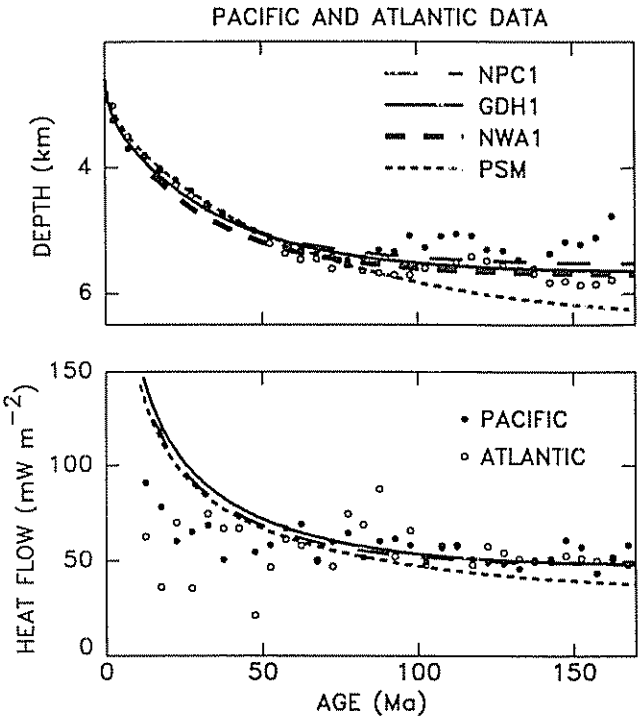

Fig. 6. Northwest Atlantic and North Pacific heat flow and depths as a function of age. Data are averaged in five-m.y. bins. Also shown are the predicted values for global models GDH1 and PSM, and models NWA1 and NPC1, each derived using data for a single ocean basin. NWA1 and NPC1 have the same predicted heat flow. The predicted depths and heat flow for the ocean-specific models closely resemble those for GDH1, indicating that GDH1 is a suitable average model for both ocean basins.

hot spot swells, plateaus, or flood basalts, is produced by processes not represented by the plate model.

The ocean-specific model parameters, and the predicted depths and heat flow, are quite similar to each other and GDH1. In particular, the predicted heat flow for GDH1 is essentially the same as for either ocean-specific model. Thus GDH1 is not unduly biased by data from one plate with respect to the other. Given the scatter in the data and the range of model parameters which give similar fits, we consider GDH1 a good compromise model for both ocean basins and data types. Hence although no reference model can fully characterize oceanic lithosphere, due to the intrinsic differences between and among ocean basins [Marty and Cazenave, 1989], GDH1 is a good approximation.

Digital Bathymetry versus Regional Median Depths

The depth data we used are from studies using the mean depths from DBDB-5 (or ETOPO-5) digital bathymetric dataset, which have some biases. To assess the effect of such biases, we compared the Pacific data to a recent set of depth data for the Pacific (Figure 7), which are computed as regional median depths taken directly from ship tracks [Smith, 1990]. These data, which span the Pacific Plate, vary with age in essentially the same way as the mean depths for the North Pacific Ocean from the digital database [Renkin and Sclater, 1988], which we used in deriving GDH1. Given that the two data sets only partially overlap in space, the agreement is gratifying. Some of the differences, such as the North Pacific being slightly deeper for young ages, may reflect the different areas sampled as much as the different data types. For older ages, where the two data sets largely sample the same area, the median depths smooth the curve, by reducing the effects of seamounts, plateaus, and other structures which bias the mean to shallower depth. As the figure illustrates, the two datasets are quite comparable, both before and after we applied an approximate sediment correction (a linear increase of sediment thickness with age rising to 300 m at 180 Ma) to Smith's data. The median absolute difference between the two datasets is approximately 130 m. The apparent difference in the uncertainties reflect Smiths' use of quartiles rather than standard deviations. Thus although the regional medians can offer better local detail and some smoothing, their overall depth-age behavior is quite comparable to the digital bathymetry, especially given the intrinsic scatter in the data.

Given that the differences between the regional medians and digital database are small compared to the differences in the thermal model predictions, we expect little difference between the lithospheric thermal structure inferred from the two. This is in fact the case. We inverted the corrected median depths by assuming a coefficient of thermal expansion of $3.1 \pm 0.8 \times 10^{-5}$ °C^{-1}, because α cannot be found independently from the basal temperature with depth data alone. The resulting model, SCD, is a 105 km thick plate with a basal temperature of 1300°C. Inversion of these depths together with the Pacific heat flow data yields model SCDH1, a 105 km thick plate with a basal temperature of 1550°C, and coefficient of thermal expansion 2.6×10^{-5} °C^{-1}. Alternatively, fixing the coefficient of thermal expansion at 3.1×10^{-5} °C^{-1} yields a poorer-fitting model, SCDH2, a 90 km thick plate with a 1375°C basal temperature. SCDH1 is almost identical from the depth-only result in its depth predictions, but also fits the heat flow. The depth-age curves for SCDH1 are similar to those for NPC1 (Figure 7), differing largely in their predictions for the young depths, and are thus similar to those for GDH1. As discussed shortly, the predicted temperature structures are also quite similar. Thus for the Pacific, the mean depths from digital bathymetry are essentially as good for depth-age studies as regional median depths.

Geoid Data

Another test of GDH1 is to examine how well it fits geoid data, which reflect a depth-weighted integral of the density distribution, and hence provide a different constraint on the geotherm from those offered by bathymetry or heat flow [Turcotte, 1986]. Lithospheric thickness as a function of age can be inferred [Crough, 1979; Sandwell and Schubert, 1982; Cazenave, 1984] from the geoid offset resulting from the age difference across fracture zones. This technique has the advantage that it suppresses the long wavelength geoid variations, and concentrates on the offset which should reflect lithospheric thickness. Figure 8 shows the fit to geoid data across a set of

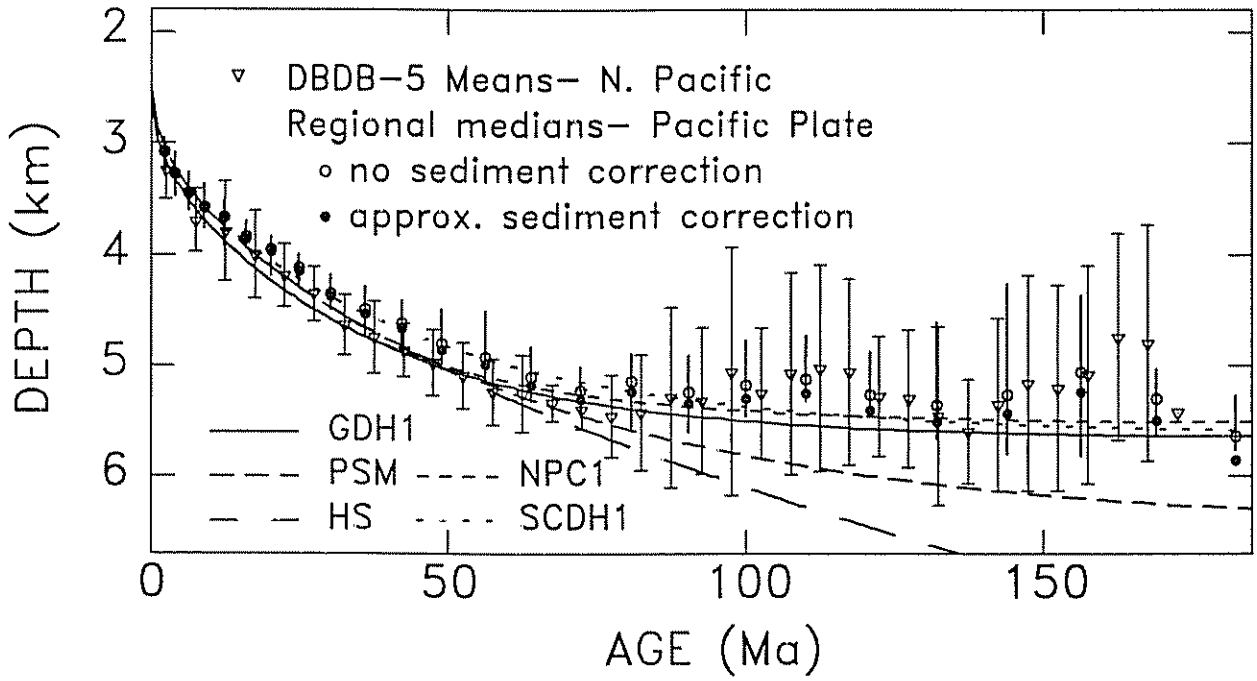

Fig. 7. Top: Comparison of different depth-age data for the Pacific. The North Pacific data [Renkin and Sclater, 1988] are mean depths, whereas the Pacific-wide data [Smith, 1990] are regional median depths from ship tracks. The data sets are quite comparable, both before and after we applied an approximate sediment correction to the median data. The apparent difference in uncertainties is because the mean depths are shown with the standard deviation, and the median depth with the quartile range. Both data sets are fit better by GDH1 than PSM. The depth-age curves for SCDH1, derived from the median depths, and NPC1, derived from the North Pacific data, are similar to each other and GDH1. The mean depths from digital bathymetry and regional median depths from ship tracks are thus essentially equivalent for our purposes.

Pacific fracture zones [Cazenave, 1984]. As noted in that paper, the data are much better fit by lithosphere thinner than the 125 km thickness for PSM. GDH1 provides a significantly better fit, but still overpredicts the geoid step, especially for young (<30 Ma) lithosphere. This misfit at the young ages may reflect the mechanics of fracture zones being more complex than a simple thermal age offset [Parmentier and Haxby, 1986; Marty et al., 1988; Driscoll and Parsons, 1988; Robinson et al., 1988; Wessel and Haxby, 1990].

Comparison of Temperature Models

The discussion of the thermal models resulting from inverting different data sets brings out the question of how to compare the models. Each model is specified by four primary parameters; the plate thickness a, basal temperature T_m, coefficient of thermal expansion α, and thermal conductivity k. The other parameters, densities, specific heat, and ridge depth are generally assumed, although the latter can also be estimated directly. For simplicity, we and others generally treat the conductivity as the same for all models. For GDH1, the improved fit from estimating the conductivity from the data is not meaningfully better than using an a priori value [Stein and Stein, 1992].

We could compare the other three parameters for different models and see whether they agree to within their difficult-to-estimate confidence limits. We instead consider it more useful to compare models in terms of those properties that are of greatest interest. As discussed earlier, such models are used primarily either to characterize depth-age and heat flow-age data, or to predict temperatures in the lithosphere. Although we fit the depth data for all ages, and the heat flow for all ages above a certain value (50 Ma), it is useful to consider three limiting features easily observable from the data. The predicted values of these features correspond to combinations of the model parameters. One such combination is the asymptotic heat flow for old lithosphere, $k\,T_m/a$, which is proportional to the asymptotic linear geotherm. A second combination is the asymptotic depth, which is proportional to $\alpha T_m a$, the heat lost as the plate cools. A third combination is the slope of the depths in young lithosphere versus the square root of age, which is proportional to $k^{1/2}\alpha T_m$. Because these depths can be equally well fit assuming a cooling halfspace, they are insensitive to plate thickness. Thus we can think of the models as having two parameters (plate thickness and basal temperatures) which reflect the thermal structure, and two parameters (conductivity and coefficient of thermal expansion) which reflect the average physical properties of the lithosphere. The latter two act as scale factors which

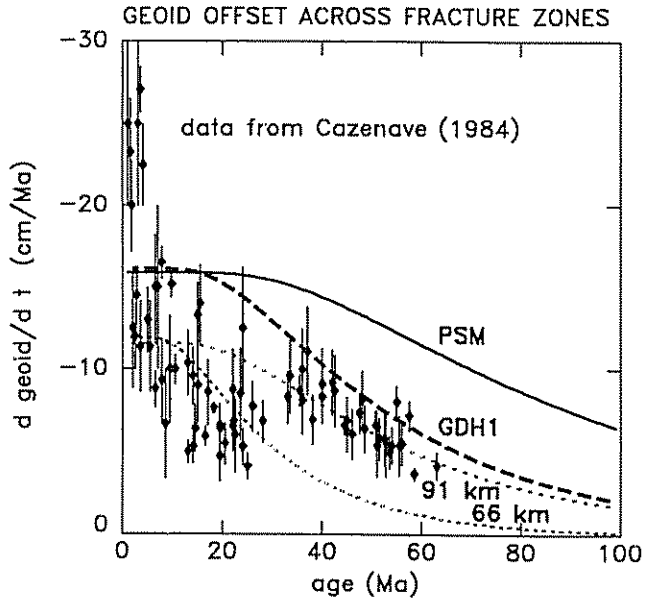

Fig. 8. Change in geoid height across Pacific fracture zones [Cazenave, 1984] and the predictions of models with different lithospheric thicknesses. The data are better fit by GDH1 than by the 125 km thickness for PSM. The remaining misfit for young (<30 Ma) lithosphere may reflect the mechanics of fracture zones being more complex than a simple thermal age offset.

map the thermal parameters into the primary observable features (young depths, old depths, and old heat flow) of the data.

Consideration of the three observable features shows why GDH1 differs from PSM in the way it does. Because GDH1 and PSM have similar predictions for the depths of young lithosphere, the product of their αT_m values must be similar. The two models have α and T_m values differing by less than 8%, and a product differing by only 4%. Thus for old lithosphere, GDH1 predicts shallower depths and higher heat flow primarily via a 24% thinner lithosphere, although the slightly higher (7%) basal temperature also contributes.

Asymptotic Depth and Heat Flow

We often compare models using the asymptotic depth and heat flow, two of the three observables used in deriving the model from the data, because both reflect the plate thickness and basal temperature. Although the asymptotic values are for infinitely old lithosphere, they are good approximations for old lithosphere. For example, the depth and heat flow predicted by GDH1 for 100 Ma lithosphere are only 154 m less and 6 mW m^{-2} higher, respectively, than their asymptotic values.

Figure 9 (top) compares the asymptotic depth and heat flow for models GDH1 and PSM to those for the ocean-specific models NWA1, NPC1 and SCDH1. PSM clearly differs significantly from these other models, which are all relatively similar to GDH1. The asymptotic depths for NWA1, NPC1 and SCDH1 are within 150 m of the 5651 m value for GDH1, whereas PSM has a noticeably deeper (6400 m) asymptotic depth. The asymptotic heat flow for these ocean-specific models is within 2 mW m^{-2} of GDH1's 48 mW m^{-2}, compared to the 34 mW m^{-2} for PSM. Some of this similarity is expected, given that the ocean-specific models were found by fitting subsets of the GDH1 heat flow data. The comparison illustrates the advantage of comparing models in terms of the asymptotic depth and heat flow. Models that are nominally different when quoted in terms of plate thickness, basal temperature, and coefficient of thermal expansion, can be quite similar in their predictions for the two observables.

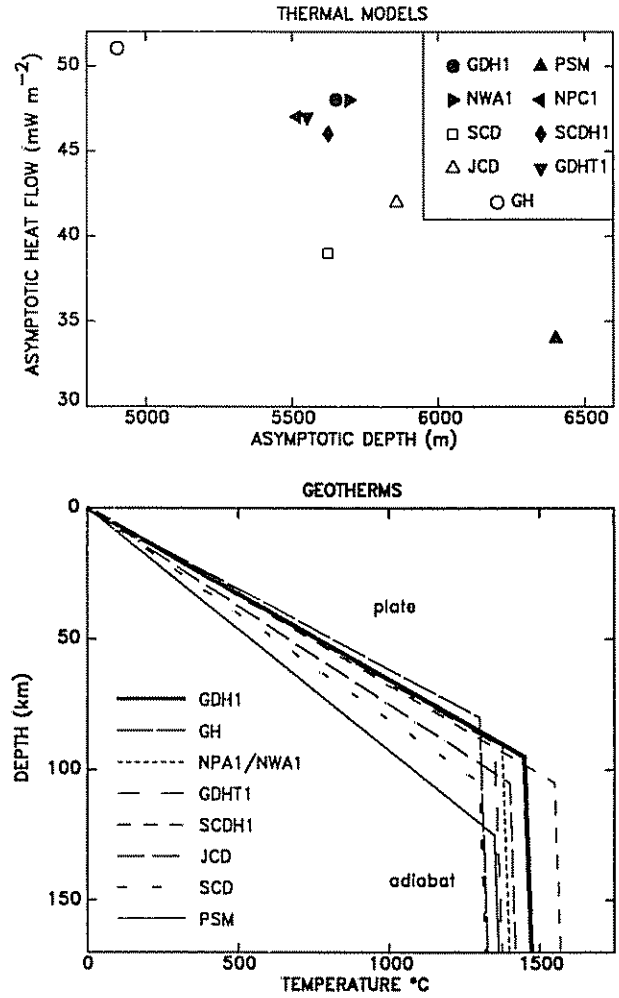

Fig. 9. Comparison of various thermal models in terms of their asymptotic depth and heat flow (top) and geotherms (bottom). In the top panel, open symbols denote models derived using either depth or heat flow data alone; closed symbols are models derived using both. Ocean-specific models derived using depth and heat flow data (NWA1, NPC1 and SCDH1) and a model derived for a 1350°C basal temperature (GDHT1) are similar to GDH1. The two models (JCD, SCD) derived using only depth data and the model derived using only global heat flow (GH) are closer to GDH1 than PSM. All models predict higher temperatures than PSM at depth within the lithosphere.

In particular, this comparison of models bears out that the differing coefficients of thermal expansion found in various inversions are features of models with similar asymptotic depth and/or heat flow. The coefficient of thermal expansion is not tightly constrained in these models, as indicated by the uncertainties estimated for GDH1 ($3.1 \pm 0.8 \times 10^{-5}$ °C^{-1}) and by Parsons and Sclater ($3.2 \pm 1.1 \times 10^{-5}$ °C^{-1}). As a result, we do not place much credence on the apparent variation in the coefficient of thermal expansion between the results of various inversions. Comparison of models SCD and SCDH1 resulting from inverting the Smith [1990] depth data with and without heat flow data illustrate that the basal temperature changed to fit the heat flow, and α changed to compensate and keep the depth prediction the same. Some of the apparent variation in α probably reflects the thermal structure of the lithosphere, and the resulting depth-age and heat flow-age variation, being more complicated than the simple plate model. The difference in the apparent α values for the Pacific models (NPC1 vs SCDH1) supports this idea.

The asymptotic depth and heat flow are useful in comparing models derived from different datasets. Johnson and Carlson's [1992] plate model was derived using only depth data, which are independent of those used in deriving GDH1. Nonetheless, as they noted, the depths predicted by their model (denoted by "JCD") are much closer to GDH1 than PSM. Similarly, inverting the Smith [1990] depth data gives model SCD, whose asymptotic depth is closer to GDH1 than PSM. If heat flow data is added to this inversion, the resulting model SCDH1 is quite similar to GDH1 in its depth and heat flow predictions. The effect of adding the heat flow data can be visualized from the position of the model (denoted by "GH") which was derived from the heat flow data alone.

We can also use this approach to see how much a model would be changed by inverting the data under different assumptions. For example, although the differences between GDH1 and PSM primarily reflect GDH1's thinner lithosphere, GDH1 also has a higher basal temperature. This 1450°C basal temperature is slightly (7%) higher than the value of approximately 1350°C often inferred for the temperature of midocean ridges from the thickness of oceanic crust [e.g. Sleep and Windley, 1982; McKenzie and Bickle, 1988]. Given the uncertainties in the GDH1 temperature (± 250°C) and in the inferred ridge temperature, it is hard to say if the difference is meaningful. The difference may be real, and reflect the basal temperature representing the heat addition to old lithosphere via mantle plumes, which are thought to be several hundred degrees hotter than the ridge temperature [Sleep, 1992]. The alternative is to ask what model results from inverting the GDH1 data, with the basal temperature fixed at 1350°C. This inversion yields model GDHT1, a 90 km thick plate with coefficient of thermal expansion 3.4×10^{-5} °C^{-1}. Also fixing α, to 3.1×10^{-5} °C^{-1}, gives a poorer-fitting model GDHT2, a 100 km thick plate. Thus, as expected, the required shallower asymptotic depths and higher asymptotic heat flow can be predicted by models with a basal temperature the same as in PSM, so long as the plate is thinner. GDHT1 and GDHT2 are quite similar to GDH1, in terms of their asymptotic depth (5552 and 5291 m) and heat flow (47 mW m^{-2}). However, the improved fit of GDH1 over these models, from also inverting for the basal temperature, is significant as measured by F-ratio test. Thus the higher basal temperature still is a better fit, at least for the data set we used. Our sense is that the thinner lithosphere will be a robust result for different data sets, but the higher basal temperature may be less so. As discussed next, we consider the hotter geotherm, corresponding to the Tm/a ratio, to be the primary feature of GDH1 and similar models.

Geotherms

Comparing models via their asymptotic depth and heat flow is a way of comparing how they fit depth and heat flow data. The asymptotic heat flow has the further advantage that it is proportional to the geotherm for old lithosphere. Given that one of our primary interests is the geotherm, we can compare the geotherms between models. The comparison is especially easy when the conductivity is assumed to be the same for different models. Figure 9 (bottom) compares the geotherms for GDH1 and PSM to those for other models. Temperatures below the plate base, which are not predicted by the models, are shown as rising along a shallow adiabatic gradient of 0.3°C km^{-1}. Although GDH1, NPC1, NWA1, SCDH1, and GDHT1 have different combinations of plate thickness and basal temperature, the geotherms are essentially the same within the lithosphere, because the models were found by fitting the heat flow data. In contrast, because PSM was found assuming lower heat flow in old lithosphere, it has a lower gradient and thus lower temperatures at any depth. Both the models derived from depth and heat flow data, and models derived from depth data alone (JCD, SCD), predict temperatures at depth higher than for PSM.

From these comparisons, we regard GDH1 as representative of the models that fit the data well. Different sets of data, and different modeling assumptions, yield different models. It would be hard to argue that one can select a "best" set of data or a "best" model. Successful models have to predict shallower asymptotic depths and higher asymptotic heat flow than PSM, and thus require higher T_m/a and lower $\alpha T_m a$, both of which can be achieved by assuming a thinner plate. We thus consider the hotter geotherm and thinner plate more important than the specific values of the basal temperature and plate thickness. Both due to the range of solutions and the simplicity of the model, we do not ascribe great significance to the details of the predicted temperature structures. This is especially the case for the thermal structure in the lower portions of the plate, beyond the general property that the models are hotter at depth than PSM.

Hot Spot Swells

The GDH1 model has major advantages for investigation of midplate volcanism and swells. Because PSM overpredicts the depth and underpredicts the heat flow for most older lithosphere, its use as a reference model has the unsatisfying implication that most of the data for older lithosphere are anomalous. This creates a situation in which apparent perturbations can result from comparing data to a model which does not appropriately represent the unperturbed lithosphere.

To illustrate this effect, we first consider the Hawaiian swell,

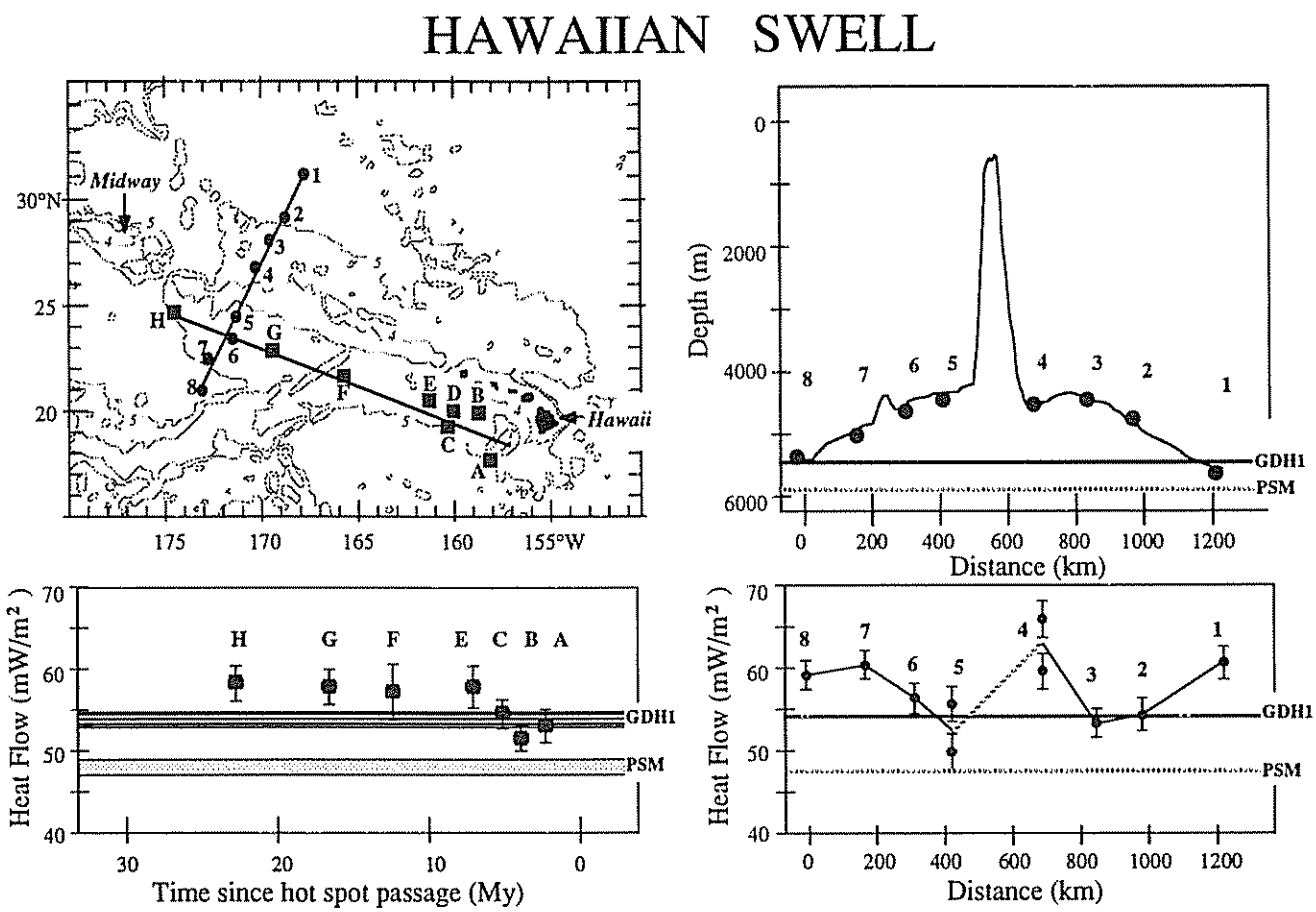

Fig. 10. Heat flow data for transects along (lower left) and across (lower right) the Hawaiian Swell at the locations shown (upper left). The heat flow, though anomalously high with respect to the Parsons and Sclater (PSM) model, is at most slightly above that expected for GDH1. The predicted heat flow values are for 100 Ma (lower right) and 95-110 Ma (lower left). Figure modified from Von Herzen et al. [1982; 1989].

the largest and best studied hot spot swell. Hawaii is the type example for hot spot studies, because of its size and isolation from other perturbing processes (including ridges and other hot spots). The observation that heat flow on the Hawaiian swell was higher than that predicted for PSM (Figure 10) was initially treated as consistent with the elevated heat flow expected for a reheating model [Von Herzen et al., 1982]. A subsequent transect across the swell showed that the heat flow differs at most slightly from that for lithosphere of comparable ages [Von Herzen et al., 1989]. Thus much of the apparent anomaly resulted from comparing the heat flow to PSM, which systematically underpredicts the heat flow for old lithosphere. In contrast, the swell heat flow is only slightly above that expected for GDH1 and hence at most slightly higher than for older lithosphere elsewhere. Even the heat flow anomaly relative to GDH1 may be an overestimate, because GDH1 slightly underpredicts the heat flow data. The swell is, of course, identified by its being shallow with respect to lithosphere of the same age elsewhere. It is thus shallow with respect to GDH1 or PSM.

The tectonic inferences that would be drawn from these data (Table 3) depend on the reference model used. Anomalies relative to a reference model are assumed to represent processes, for example plumes, not included in the reference model assumptions. Because both the depths and the heat flow are significantly anomalous with respect to PSM, one would infer that the hot spot gives rise to additional heat flow and shallow topography. In contrast, using GDH1 implies that the uplift has little heat flow signature, suggesting that the topography results primarily from dynamic effects. Hence the plume is providing uplift beyond that observed for most lithosphere of this age. These data can thus be used as modeling constraints [e.g. Von Herzen et al., 1982; Liu and Chase, 1989]. The interpretation that the Hawaiian swell heat flow data favor a dynamic model is consistent with seismological data, which find no evidence for a low velocity zone under the swell [Woods et al., 1991].

A similar situation applies for the Bermuda, Cape Verde and Crozet hot spot swells (Figures 11, 12, and 13). The heat flow data [Detrick et al., 1986; Courtney and White, 1986; Courtney

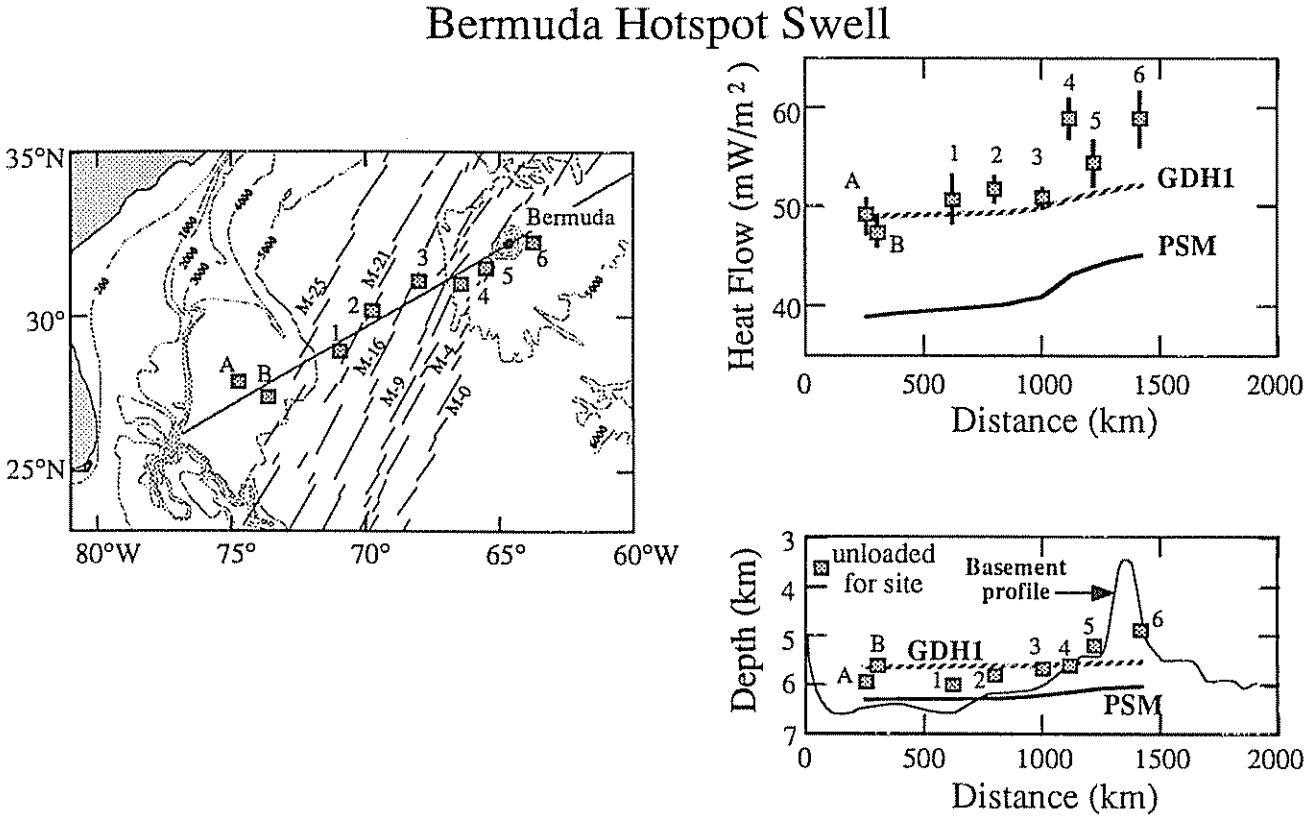

Fig. 11. Heat flow data and depth data for the Bermuda Swell. The heat flow data [Detrick et al., 1986] show a large anomaly with respect to PSM, but a much smaller one with respect to GDH1.

and Recq, 1986] show a large anomaly with respect to PSM, but a much smaller one with respect to GDH1.

The fractions of thermal and dynamic uplift can be estimated crudely [Sleep, 1990] by using the observed heat flow to determine the thermal age, the age at which a reference model predicts the observed heat flow. We then find the thermal depth anomaly, the difference between the predicted depth for the thermal age and that observed, and compare it to the total depth anomaly, the difference between the predicted depth for the lithospheric age and that observed. Table 4 shows these estimates, illustrating that GDH1 predicts higher heat flow and hence less thermal uplift than PSM.

We consider the estimates of the thermal uplift fraction crude for several reasons. The thermal uplift fraction is an lower bound, in that some of the perturbed heat flow may not yet be detectable at the surface, so the thermal age is an upper bound assuming the data and reference model were known exactly. In fact, both the data and model have uncertainties. Thus the thermal uplift fraction estimates depend on the assumed values of the swell depth (taken here from Detrick et al. [1989]) and heat flow. In addition, the estimates depend on the assumed depth and heat flow for "normal" lithosphere, which although predicted better by GDH1 than PSM, still have uncertainties. Nonetheless, it appears that the data favor a primarily dynamic origin for the swells. The dynamic component is 2-3 times larger than would be inferred using the PSM reference model. We thus regard these estimates as illustrating how improved reference models like GDH1 can be useful in studies using more sophisticated models of hot spots.

Darwin Rise Depth and Heat Flow

To determine whether the Darwin Rise retains a thermal anomaly at present from the process which caused the widespread Cretaceous volcanism and uplift, we examined the depth and heat flow data [Stein and Abbott, 1991]. For this purpose, the Darwin Rise was assumed to be the region (Figure 2) surrounding the continuation of hot spot tracks from the present-day Superswell, an area roughly south and west of Hawaii and north of the Samoan hot spot track. The heat flow data for the sites, averaged in 20 m.y. bins, are shown in Figure 14. The Darwin Rise heat flow values are anomalously high with respect to PSM, but consistent with GDH1.

In addition, the Darwin Rise data can be compared directly with data from the rest of the Pacific plate. In each of the age bins the difference of the means between the Darwin Rise data and that elsewhere in the Pacific is less than 10 mW m^{-2} and the maximum difference in median value is 7 mW m^{-2}. The Darwin Rise data thus show no evidence for a heat flow ano-

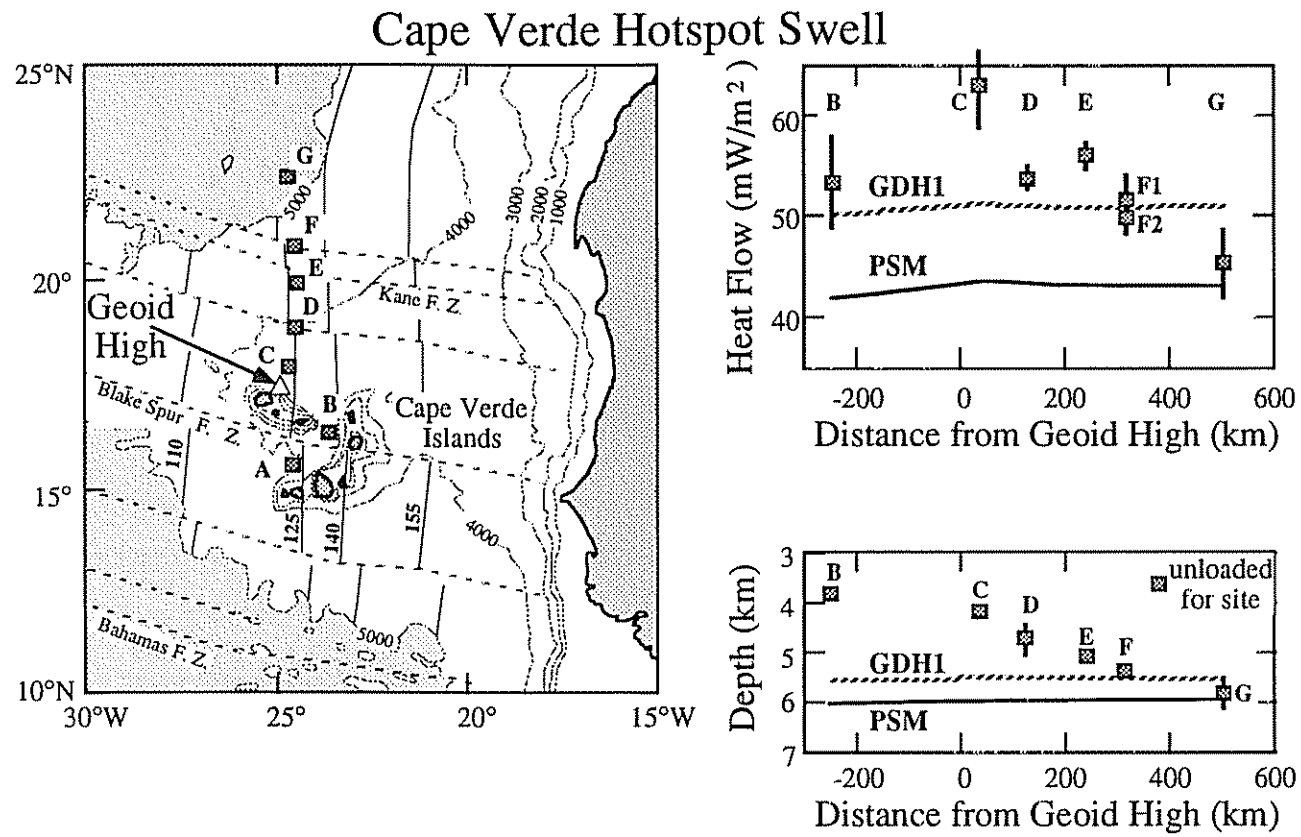

Fig. 12. Heat flow data and depth data for the Cape Verde Swell. The heat flow data [Courtney and White, 1986] show a large anomaly with respect to PSM, but a much smaller one with respect to GDH1.

maly either relative to lithosphere of these ages elsewhere in the Pacific, or the global dataset. Moreover, the lack of an anomaly is not a result of some condition specific to the Pacific Plate, because the predicted heat flow for the model derived from the Atlantic data alone (Figure 6) is essentially the same as for GDH1. Direct comparison with the Atlantic data also shows no anomaly [Stein and Abbott, 1991].

The Darwin Rise has been considered anomalously shallow, based on comparisons with the PSM model [Schlanger and Premoli-Silva, 1981; McNutt et al., 1990]. This interpretation implies that the area is characterized not only by many seamounts, but by a regional bathymetric anomaly. To test this idea, we compared the depths of the Darwin Rise heat flow sites to those elsewhere in Pacific, and to the two reference models. The depths in Figure 14 differ from those shown by Stein and Abbott [1991] because we corrected for sediment thickness, using seismic reflection records for 128 sites and isopachs [Ludwig and Houtz, 1979] for the remaining 135.

The depths are anomalously shallow with respect to PSM, but are consistent with GDH1. Similarly, the depths are comparable to those of lithosphere for these ages elsewhere in the Pacific. (The shallow average depth for the 135-155 Ma data elsewhere in the Pacific is due to sites on the Hess and Shatsky Rises and the Ontong-Java Plateau). We thus find no evidence for the Darwin Rise being anomalously shallow, either with respect to the rest of the Pacific or GDH1.

The lack of depth and heat flow anomalies has interesting implications for the history of the Darwin Rise. McNutt et al. [1990] (Figure 15) inferred that the Darwin Rise was similar to the present Superswell, which they assume to be characterized by an anomalously thin plate, and thus subsided at a slow rate from its formation (113 ± 8 Ma) until about 70–80 Ma, after which it subsided at the rate of normal seafloor. The present depth, which was interpreted as anomalously shallow with respect to PSM, would thus indicate that the thermal structure differs from that of comparable age lithosphere elsewhere. In contrast, we find no depth anomaly with respect to GDH1, and thus no evidence for the Rise lithosphere presently retaining a significant thermal signature of the Cretaceous events.

SUPERSWELL DEPTH AND HEAT FLOW

We conducted a similar depth and heat flow analysis for the Superswell. The heat flow sites in the area [Stein and Abbott, 1991] provide good regional coverage of the Superswell and, for comparison, the region surrounding it. The sites sample the region of shallower bathymetry described by McNutt and Fisher [1987].

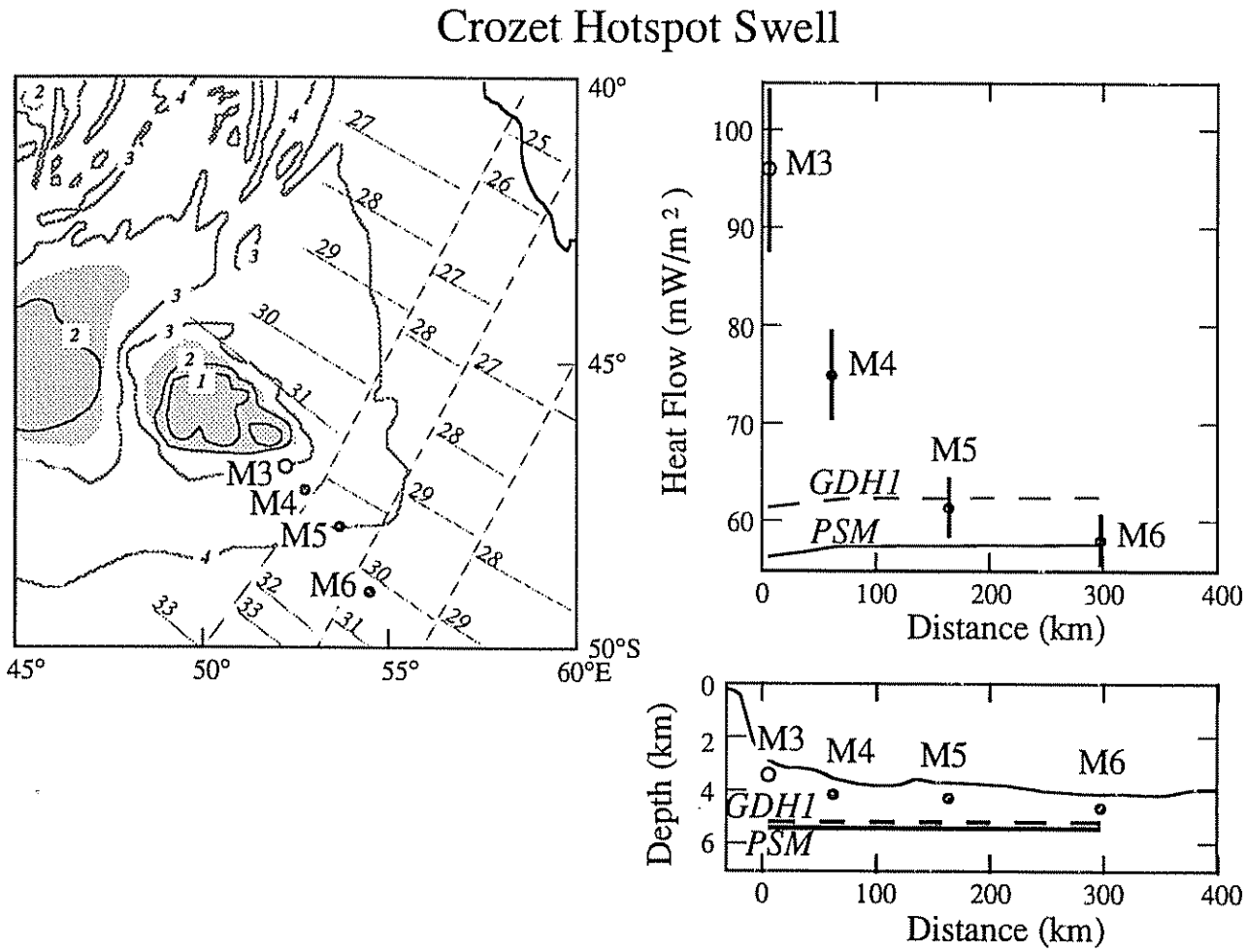

Fig. 13. Heat flow data and depth data for the Crozet Swell. The heat flow data [Courtney and Recq, 1986] show a smaller anomaly with respect to GDH1 than PSM. The magnitude of the anomaly estimated in Table 4 depends on whether the swell heat flow is assumed to be that for site M3 or M4; the M3 value is from one measurement and was thus not considered very reliable by Courtney and Recq.

Figure 16 shows the heat flow data versus age for the Superswell region and elsewhere on the Pacific plate. The data are divided into four age bins, each containing an approximately equal number of data for the Superswell. Comparison with GDH1 shows the characteristically lower than predicted heat flow for young (<50 Ma) lithosphere, that is observed elsewhere (Figure 3) and presumably reflects hydrothermal circulation. For the older ages, the data show no anomaly with respect to GDH1. Similarly, the heat flow values for the Superswell are no higher than for the corresponding ages elsewhere on the Pacific plate. The heat flow data thus neither require nor exclude the possibility of a thinner thermal lithosphere, as shown by predictions for the 75 km-thick plate with a 1385°C basal temperature suggested by McNutt and Fisher [1987]. The poor fit of the heat flow for ages > 60 Ma predicted by a 60 km-thick plate argues against further thinning.

The depth data provide another constraint. As shown, the depths are shallower than expected for GDH1. The depths in Figure 16 differ from those shown by Stein and Abbott [1991] because we corrected for sediment thickness, using seismic reflection records for 112 sites and isopachs [Ludwig and Houtz, 1979] for the remaining 245. The Superswell heat flow sites are shallower than sites of the same age elsewhere on the Pacific plate. The depths shown here for a model with a 75 km plate are somewhat deeper than shown by McNutt and Fisher [1987] and Stein and Abbott [1991] because we use a formulation in which the ridge depth is fixed to the observed value [Stein and Stein, 1992]. In the other formulation, the ridge depth varies depending on the temperature structure, and is thus shallower for hotter plates [McNutt and Fisher, 1987]. The subsidence with respect to the ridge, which reflects the cooling, is the same in both formulations. GDH1, which corresponds to a thicker plate, better fits the depth of the other Pacific sites.

The depth and heat flow situation for the Superswell is thus

TABLE 4: Hotspot Thermal Anomaly Estimates

	Thermal age	Thermal depth anomaly	Thermal fraction of total depth anomaly
Hawaii (lithospheric age 100 Ma; heat flow 58 mW m^{-2})			
PSM	67 Ma	449 m	37 %
GDH1	81 Ma	106 m	12 %
Bermuda (lithospheric age 116 Ma; heat flow 58 mW m^{-2})			
PSM	67 Ma	595 m	69 %
GDH1	81 Ma	161 m	36 %
Cape Verde (lithospheric age 125 Ma; heat flow 62 mW m^{-2})			
PSM	59 Ma	819 m	43 %
GDH1	69 Ma	285 m	19 %
Crozet (lithospheric age 67 Ma; heat flow 75-96 mW m^{-2}*)			
PSM	40-24 Ma	593-1081 m	21-39 %
GDH1	46-28 Ma	299-745 m	11-28 %

*Values given assuming that the swell heat flow is that for either site M3 or M4; the higher (M3) value was considered less reliable.

similar in general to that for Hawaii (Figure 10), in that the shallow depth anomaly has no corresponding high heat flow anomaly. The Superswell has drawn such interest, however, because of the large area over which the depth anomaly extends. Much of this depth anomaly might be expected simply from the fact that the Superswell region contains a number of hot spot swells. McNutt and Fisher [1987] and McNutt and Judge [1990], however, find that a depth anomaly remains even after removal of the estimated effects of the swells, and interpret the residual anomaly as evidence for dynamic uplift by a large scale plume.

The depth and heat flow anomaly data for the Hawaiian swell, the Superswell, and the Darwin Rise thus are generally consistent. The present swells, Hawaii and the Superswell, show significant depth but at most minimal heat flow anomalies, implying that the uplift is primarily dynamic. The Darwin Rise shows neither a heat flow anomaly nor a depth anomaly, suggesting that the effects of the Cretaceous volcanism have dissipated.

Flexural Data

The flexural data for these three regions, however, are inconsistent and more challenging to interpret. The strength of the lithosphere can be inferred from the shape of the deflection induced by the loads of seamounts and islands. The effective elastic thickness, a representation of the vertically integrated strength when the load was applied, generally increases approximately as the square root of the loading age [Watts et al., 1980], and corresponds to depths where the predicted temperatures are approximately 300-600°C (Figure 17) [Bodine et al., 1981]. These observations are consistent with ductile flow laws in which strength decreases exponentially with temperature [Kirby, 1977, 1980; Goetze and Evans, 1979], because cooling of the lithosphere would give increased strength at depth.

The effective elastic thicknesses beneath islands and seamounts in the Superswell and Darwin Rise are anomalously low for their age of loading (Figure 17) compared with sites along the Hawaiian swell, elsewhere in the Pacific, or in the Atlantic and Indian Oceans. It has been suggested that the low effective elastic thicknesses for the Superswell and Darwin Rise reflect weakening due to elevated temperatures in the lithosphere [Menard and McNutt, 1982; Calmant and Cazenave, 1987; McNutt and Fisher, 1987; Smith et al., 1989; McNutt and Judge, 1990]. This idea can be tested via the simple assumption

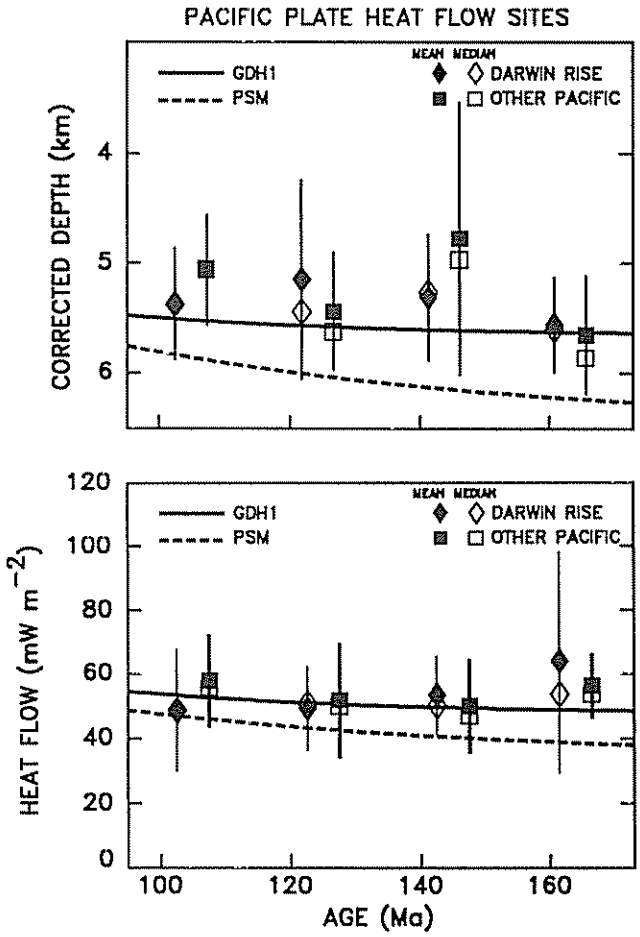

Fig. 14. Depth (top), and heat flow (bottom) as a function of age for sites on the Darwin Rise and on lithosphere of the same age elsewhere in the Pacific. Data are averaged in 20-m.y. bins. The depths and heat flow, though anomalously shallow and high, respectively, relative to PSM, are consistent with GDH1. Because the Darwin Rise data also do not differ significantly from those for the remainder of the Pacific, the Rise appears not to be anomalously shallow or hot at present.

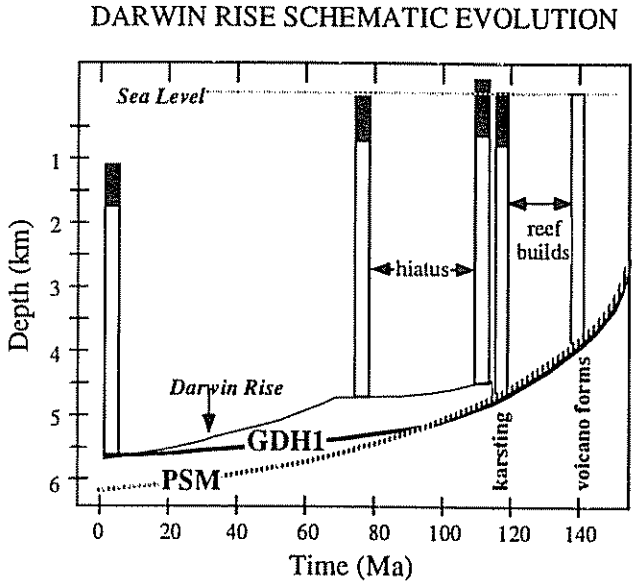

Fig. 15. Schematic history for the Darwin Rise [McNutt et al., 1990], for the case of a 140-Ma volcano on 155-Ma lithosphere. The Darwin Rise is presently anomalously shallow with respect to PSM, but not with respect to GDH1, suggesting that the Rise presently does not retain a significant thermal signature of the Cretaceous events.

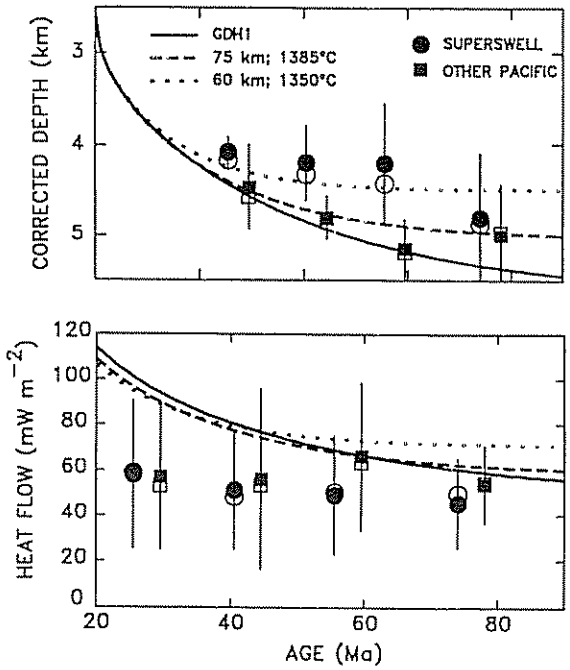

Fig. 16. Corrected depth (top), and heat flow (bottom) as a function of age for sites in the Superswell and on lithosphere of the same age elsewhere in the Pacific. Data are averaged in 20-m.y. bins. Closed and open symbols indicate means and medians, respectively. For ages >50 Ma the Superswell heat flow data do not differ significantly from those for the remainder of the Pacific or from those expected for GDH1. The Superswell depths are shallower than for the remainder of the Pacific, or than expected for GDH1.

that if the thinner effective elastic thicknesses result from thermal perturbations, the perturbed 300° and 600°C isotherms should rise to corresponding depths.

Figure 17 shows the predicted depths of the isotherms for GDH1 and the 75-km-thick plate proposed by McNutt and Fisher [1987]. The depths to the isotherms in the upper lithosphere for the 75-km-thick plate are only slightly shallower, because of the relatively young ages at the time of loading for the Superswell. This elevation of the isotherms should produce little change in effective elastic thickness.

Alternatively, much more dramatic heating could reduce the effective elastic thickness to that observed. The required high temperatures, however, appear to be excluded by the heat flow and depth data. Figure 18 (top) shows that a 40-km-thick plate with a 1350°C basal temperature or a 75-km-thick plate with a 2000°C basal temperature would have 400°C isotherms shallow enough to be consistent with the Superswell and Darwin Rise effective elastic thicknesses. Such models, however, predict heat flow substantially greater than observed (Figure 18, bottom) and seafloor depths much shallower than observed [Stein and Abbott, 1991].

These calculations are for steady state models, in which the boundary conditions do not change. An alternative approach is to consider models in which the thermal structure of the lithosphere is perturbed and then evolves. Figure 19 shows the temperature structure and heat flow predicted by a halfspace reheating model in which the base of the lithosphere is reset to asthenospheric temperatures and then cools [Von Herzen et al., 1982] The reheating depth determines the anomalous bathymetry

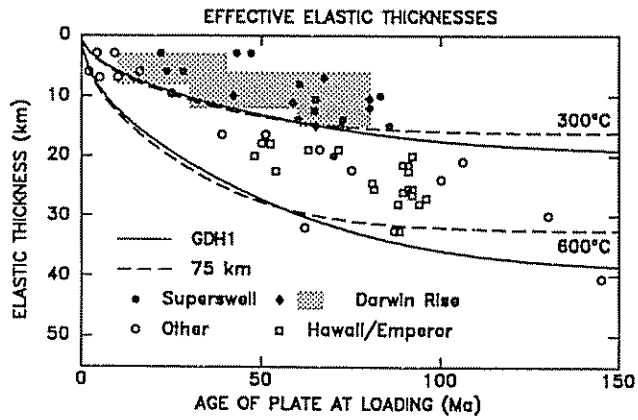

Fig. 17. Effective elastic thicknesses for locations on the Superswell and Darwin Rise compared to sites elsewhere. Data compiled from Smith et al. [1989], Calmant et al. [1990], and Wolfe and McNutt [1991] (shaded area). The thicknesses for the Darwin Rise and Superswell are less than for the other regions, including the Hawaiian Swell. Isotherms predicted for model GDH1 and for a model with a 75 km thick plate are also shown.

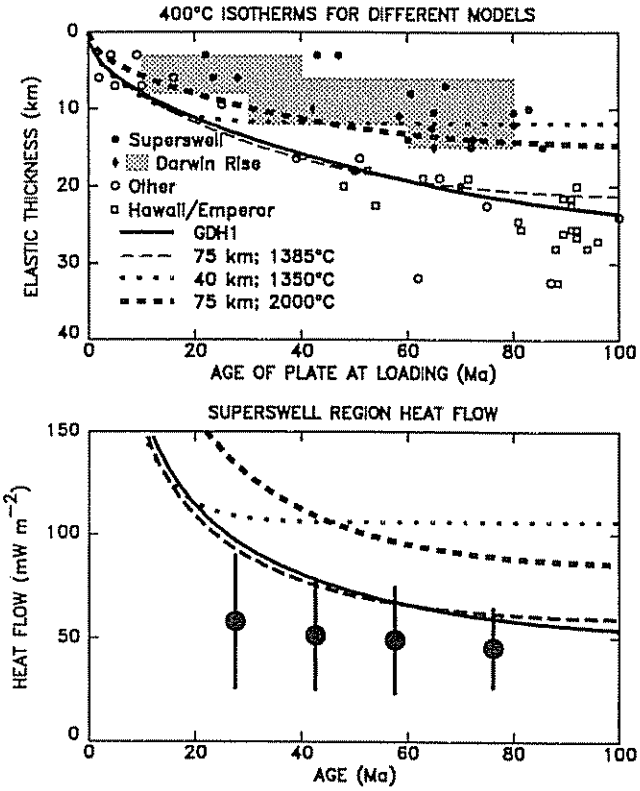

Fig. 18. Comparison of observed effective elastic thicknesses and predicted isotherms for various models. Effective elastic thicknesses for areas other than the Superswell and Darwin Rise correspond approximately to the GDH1 400°C isotherm. Models which raise the temperatures enough to make the Superswell thicknesses correspond to the 400°C isotherm (top) would yield heat flow much higher than observed for the Superswell (bottom).

and heat flow with time: the shallower the reheating depth, the greater the depth anomaly, the sooner the maximum surface heat flow anomaly occurs, and the greater its magnitude. Reheating 45-Ma lithosphere to the depth of the 900°C isotherm, as proposed by McNutt [1987], results in too little shallowing of the 400°C isotherm to explain the flexural data. Much shallower reheating is required to elevate the temperatures sufficiently to fit the effective elastic thicknesses data. In this example, thinning to 15 km depth would be required to place the effective elastic thicknesses in the expected temperature range. Such thinning would cause much higher heat flow than observed.

These results are interesting for the comparison with the Hawaiian swell. For Hawaii, the lack of a heat flow anomaly precludes major reheating of the lithosphere, an inference which is also consistent with the normal effective elastic thickness values. For the Superswell, although the effective elastic thicknesses indicate anomalously weak lithosphere, the heat flow excludes significant reheating. Thus the difference between the small effective elastic thicknesses for the Superswell and Darwin Rise and the larger values for Hawaii and the other regions appears not to result from general thermal weakening of the entire lithosphere.

There are several obvious other possibilities for the mechanism causing the Superswell and Darwin Rise lithosphere to have thinner effective elastic thicknesses than the other swells [Stein and Abbott, 1991]. First, shallow reheating might be localized under the seamounts, and thus not reflected in the heat flow data. This seems unlikely, given that the Superswell appears to be a widespread phenomenon. Second, the weakness might be only apparent, due to the action of intraplate stresses. Third, the lithosphere might be weakened mechanically.

In the second case, the low effective elastic thicknesses could reflect intraplate stresses. The flexural response of the lithosphere to an applied load depends on both the mechanical properties and the intraplate stress. Figure 20 (top) shows this effect schematically for a line seamount load on a 20 km thick elastic plate, computed using the formulation of Hetenyi [1974]. 500 MPa (5 Kb) of compressional stress reduces the effective elastic thickness to 16 km, and a 1 GPa (10 Kb) stress reduces it to 14 km. The high stresses in this elastic example would be less for a realistic depth dependent rheology [McAdoo and Sandwell, 1985]. McNutt et al [1991], for example, propose that approximately 50 MPa of in-plane tension could explain the Superswell effective elastic thicknesses.

This hypothesis is difficult to test, in that the relevant intraplate stress is that at the time of loading. There is, however, no apparent reason to expect the effect of regional intraplate stresses to have been dramatically greater for the Superswell than for other swells. The present intraplate seismicity is not particularly intense [Wysession et al., 1991], especially in terms of large events, and the present intraplate stresses predicted from driving force models are not unusually high [Wortel et al., 1991]. This situation is quite different from the Indian Ocean, where large earthquakes occur [Stein and Okal, 1978; Bergman and Solomon, 1985] and the predicted high stresses [Cloetingh and Wortel, 1985, 1986; Stein et al., 1987] are consistent with the observed large scale deformation [Stein et al., 1989]. In principle, the Superswell-forming process might instead somehow have provided the necessary stresses. It is unclear, however, how this might occur. Although hot spots might give rise to significant thermal stresses [Zhu and Wiens, 1991], these stresses should occur for all hot spots, not just those in the Superswell. We thus have difficulty envisioning how the apparent differences in lithospheric strength between the Superswell and other swells could be a consequence of intraplate stress.

An alternative possibility is that the lithosphere beneath the Superswell and Darwin Rise have been weakened mechanically, giving rise to a lower effective elastic thickness. Figure 20 (bottom) illustrates this schematically for the limiting case of a fractured lithosphere: a broken 20 km thick plate looks quite similar to an unbroken 11 km thick plate with the same physical properties. Hence an analysis which assumed that the lithosphere was not broken would yield an 11 km effective elastic thickness. In such a scenario, the weakening might occur in several ways [Stein and Abbott, 1991]. The Superswell-forming

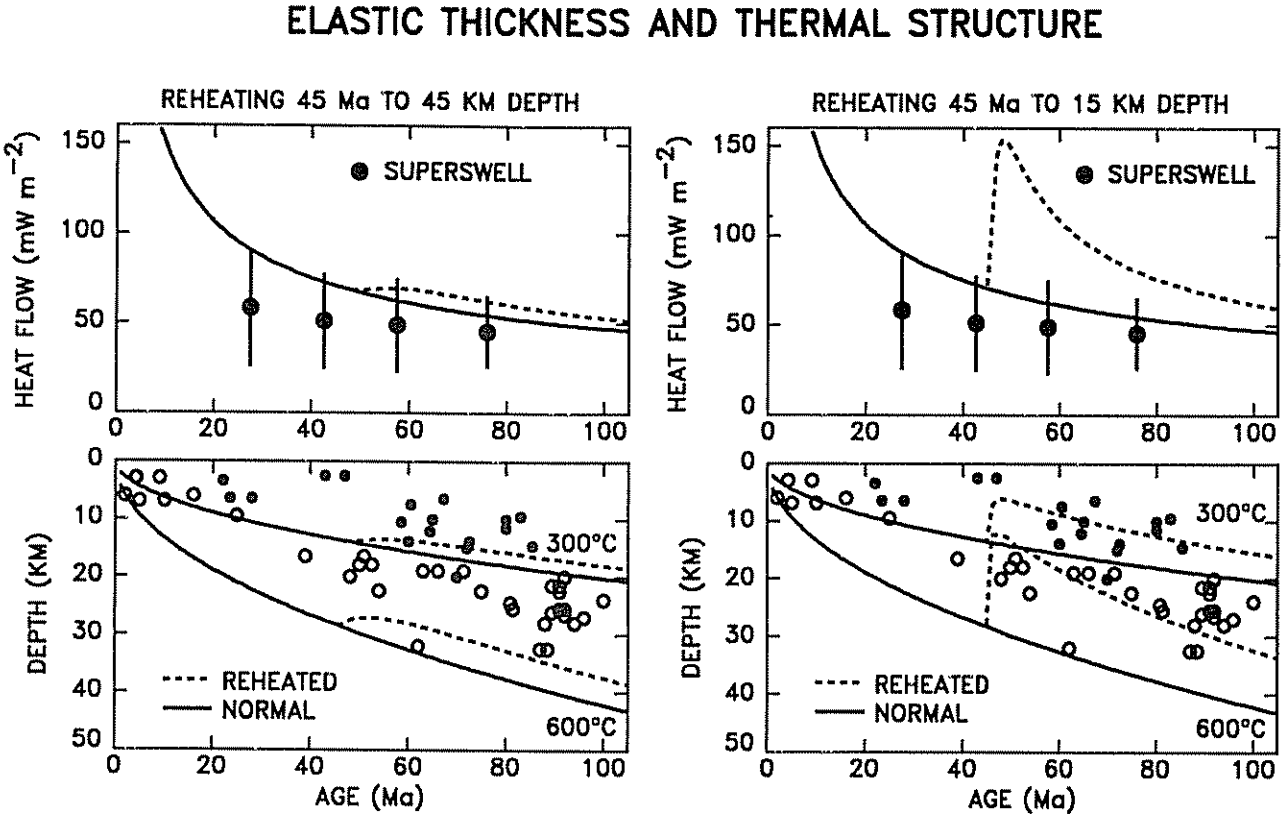

Fig. 19. Application of reheating models to the Superswell heat flow and effective elastic thickness data. Superswell seamount chains are indicated by closed symbols; other chains are shown as open symbols. Right: Model for reheating 45-Ma lithosphere to a depth of 45 km. Although the calculated heat flow anomaly (top) is plausible given the observed heat flow, such a model does not give sufficient reheating of the upper lithosphere (bottom) to account for the low effective elastic thicknesses. Left: Model for reheating 45-Ma lithosphere to a depth of 15 km. Although this model produces sufficient reheating in the upper lithosphere to account for the effective elastic thicknesses of the superswell sites, it predicts a heat flow anomaly significantly larger than that observed. [Stein and Abbott, 1991].

process might introduce significant amounts of volatiles such as water, giving rise to the weaker rheology expected from laboratory experiments [Kirby, 1983]. Alternatively, weakening might be due to successive intrusion events cracking and flexing the lithosphere [Diament and Baudry, 1987].

This hypothesis has the advantage that the unusual weakness in the Superswell area is related to the area's history. Given the Superswell's complex history of volcanism due at least in part to multiple hot spots, it is conceivable that the hot spots and possible Superplume have affected the lithosphere in the way required. The difficulty with this idea, however, is that it is hard to test. We can exclude general thermal weakening from the absence of its observable consequences for heat flow and depth and the absence of evidence from mantle xenoliths for high lithospheric temperatures [Tracy, 1980]. In contrast, a mechanically weakened lithosphere would be difficult to observe except in the flexural data that lead to the suggestion of this property. Although in principle earthquake depths might constrain the weakening [Wiens and Stein, 1983; Liu and Chase, 1989], the low level of seismicity makes such analysis difficult.

Conclusions

Because much of the data on the processes giving rise to midplate swells and volcanism are derived from depth and heat flow anomalies, the choice of the reference model with respect to which these anomalies are computed is significant. GDH1, a reference model which describes the depth and heat flow in older lithosphere reasonably well, thus is helpful in assessing anomalies. In particular, it indicates that heat flow in swell regions, which previously appeared anomalously high, is at best slightly higher than for lithosphere of the same age elsewhere. This observation tends to favor largely dynamic, rather than thermal, models for swell uplifts. It similarly excludes the possibility that the weak lithosphere inferred for the Superswell results from elevated temperatures.

More generally, these results bear out the desirability of

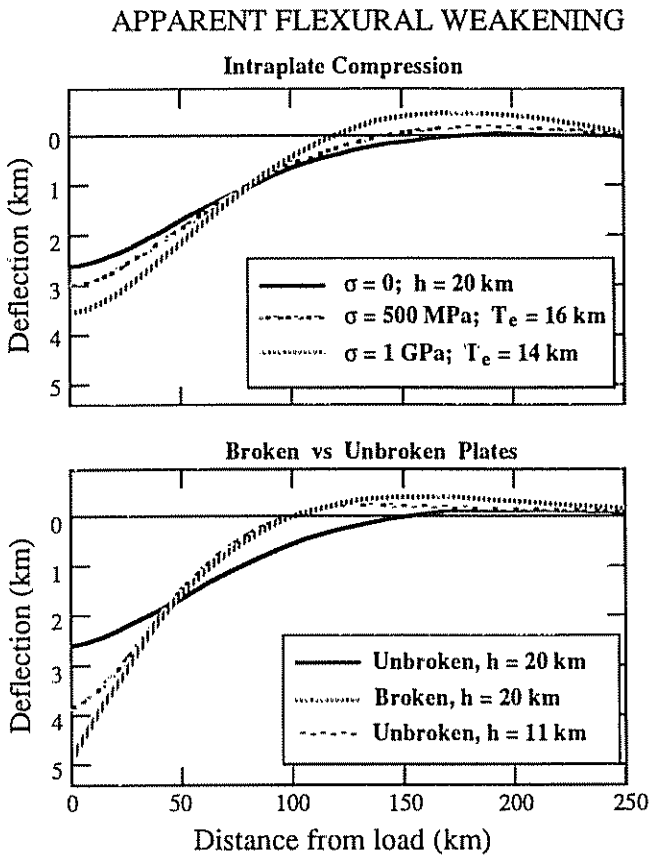

Fig. 20. Schematic illustration of two possible models for apparent weakening of the lithosphere, as inferred from flexural data. Top: Deflection of a 20 km thick lithosphere assuming different values of intraplate compression. Larger stresses reduce the effective elastic thickness, T_e. Bottom: Deflection of 20 km thick lithosphere, for unbroken and broken cases. The effective elastic thickness inferred from the flexural shape for the broken lithosphere would be 11 km.

developing improved reference models, both for comparison with observable data and for interpretation of the corresponding anomalies in temperature and physical properties in the lithosphere. It is worth noting that this situation is a common one in the earth sciences. For example, corresponding reference model artifacts occur in seismology, where an inappropriate velocity reference model can produce apparent anomalies [van der Hilst and Spakman, 1989].

Acknowledgments. Our thinking about midplate swells was influenced greatly by many pleasant discussions with Sy Schlanger. We learned much from his deep familiarity with a wide range of data, his interest in treating the data as constraints on large scale tectonic processes, and his geological intuition. For example, when we told him why we favored mechanical rather than thermal weakening of the Superswell lithosphere, Sy said he had long believed that seamounts weakened the plate as they erupted, and that their loads should not be treated "as though they were dropped from balloons." Sy was a fine scientist, a warm person, and a good friend.

We thank Aristeo Pelayo for assistance in preparing the figures, Richard Carlson, Paul Johnson, Norm Sleep, Tom Shoberg, and Mark Woods for helpful discussions, and Clem Chase and Cecily Wolfe for useful reviews. This research was supported by NSF grant OCE-9019572 and NASA grant NAG-5-1944.

REFERENCES

Anderson, R. N., and M. A. Hobart, The relation between heat flow, sediment thickness, and age in the eastern Pacific, *J. Geophys. Res.*, *81*, 2968–2989, 1976.

Anderson, R. N., and J. N. Skilbeck, Oceanic heat flow, in *Oceanic Lithosphere, The Sea, 7*, edited by C. Emiliani, pp. 489–523, Wiley-Interscience, New York, 1981.

Bergman, E. A., and S. C. Solomon, Earthquake source mechanisms from body waveform inversion and intraplate tectonics in the northern Indian Ocean, *Phys. Earth Planet. Inter., 40*, 1–23, 1985.

Bodine, J. H., M. S. Steckler, and A. B. Watts, Observations of flexure and the rheology of the oceanic lithosphere, *J. Geophys. Res., 86*, 3695–3707, 1981.

Buck, W. R., and E. M. Parmentier, Convection beneath young oceanic lithosphere: implications for thermal structure and gravity, *J. Geophys. Res., 91*, 1961–1974, 1986.

Calmant, S., The elastic thickness of the lithosphere in the Pacific Ocean, *Earth Planet. Sci. Lett., 85*, 277–288, 1987.

Calmant, S., and A. Cazenave, Anomalous elastic thickness of the oceanic lithosphere in the south-central Pacific, *Nature, 328*, 236–238, 1987.

Calmant, S., J. Francheteau, and A. Cazenave, Elastic layer thickening with age of the oceanic lithosphere a tool for prediction of age of volcanoes or oceanic crust, *Geophys. J. Int., 100*, 59–67, 1990.

Castillo, P., The Dupal anomaly as a trace of the upwelling lower mantle, *Nature, 336*, 667–670, 1988.

Cazenave, A., Thermal cooling of the lithosphere: new constraints from geoid height data, *Earth Planet. Sci. Lett., 70*, 395–406, 1984.

Chen, W.-P., and P. Molnar, Focal depths of intracontinental and intraplate earthquakes and their implications for the thermal and mechanical properties of the lithosphere, *J. Geophys. Res., 88*, 4183–4214, 1983.

Cloetingh, S., and R. Wortel, Regional stress field of the Indian plate, *Geophys. Res. Lett., 12*, 77–80, 1985.

Cloetingh, S., and R. Wortel, Stress in the Indo-Australian plate, *Tectonophysics, 132*, 49–67, 1986.

Cochran, J. R., Variations in subsidence rates along intermediate and fast spreading mid-ocean ridges, *Geophys. J. R. astron. Soc., 87*, 421–454, 1986.

Colin, P., and L. Fleitout, Topography of the ocean floor: Thermal evolution of the lithosphere and interaction of deep mantle heterogeneities with the lithosphere, *Geophys. Res. Lett., 17*, 1961–1964, 1990.

Courtney, R. C., and M. Recq, Anomalous heat flow near the Crozet Plateau and mantle convection, *Earth Planet. Sci. Lett., 79*, 373–384, 1986.

Courtney, R. C., and R. S. White, Anomalous heat flow and geoid across the Cape Verde Rise: evidence for dynamic support from a thermal plume in the mantle, *Geophys. J. R. astron. Soc., 87*, 815–867, 1986.

Crough, S. T., Approximate solutions for the formation of the lithosphere, *Phys. Earth Planet. Inter., 14*, 365–377, 1977.

Crough, S. T., Thermal origin of mid-plate hot-spot swells, *Geophys. J. R. astron. Soc., 55*, 451–469, 1978.

Crough, S. T., Geoid anomalies across fracture zones and the thickness of the lithosphere, *Earth Planet. Sci. Lett., 44*, 224–230, 1979.

Darwin, C., *The Voyage of the Beagle (1975 reissue)*, J. M. Dent, London, 1845.

Davies, G. F., Ocean bathymetry and mantle convection, 1. Large-scale flow and hot spots, *J. Geophys Res., 93*, 10,467–10,480, 1988.

Davies, G. F., and F. Pribac, Mesozoic seafloor subsidence and the Darwin Rise past and present, this volume.

Davis, E. E., and C. R. B. Lister, Fundamentals of ridge crest topography, *Earth Planet. Sci. Lett., 21*, 405–413, 1974.

Detrick, R. S., and S. T. Crough, Island subsidence, hot spots, and lithospheric thinning, *J. Geophys. Res., 83*, 1236–1244, 1978.

Detrick, R. S., R. P. Von Herzen, B. Parsons, D. Sandwell, and M. Dougherty, Heat flow observations on the Bermuda Rise and thermal models of midplate swells, *J. Geophys. Res., 91*, 3701–3723, 1986.

Detrick, R. S., R. S. White, R. C. Courtney, and R. P. Von Herzen, Heat flow on midplate swells, in *Handbook of seafloor heat flow*, edited by J. A. Wright and K. E. Louden, pp. 325–485, CRC Press, Inc., Boca Raton, Florida, 1989.

Diament, D., and N. Baudry, Structural trends in the Southern Cook and Austral archipelagoes (south central Pacific) based on an analysis of Seasat data: Geodynamic implications, *Earth Planet Sci. Lett., 85*, 427–438, 1987.

Driscoll, M. L., and B. Parsons, Cooling of the oceanic lithosphere - evidence from geoid anomalies across the Udintsev and Eltanin fracture zones, *Earth Planet. Sci. Lett., 88*, 289–307, 1988.

Duncan, R. A., and D. A. Clague, Pacific plate motion recorded by linear volcanic chains, in *The Ocean Basins and Margins, 7A: The Pacific Ocean*, edited by A. E. Nairn, F. G. Stehli and S. Uyeda, pp. 89–121, Plenum Press, New York, 1985.

Forsyth, D. W., The evolution of the upper mantle beneath mid-ocean ridges, *Tectonophysics, 38*, 89–118, 1977.

Goetze, C., and B. Evans, Stress and temperature in the bending lithosphere as constrained by experimental rock mechanics, *Geophys. J. R. astron. Soc., 59*, 463–478, 1979.

Hager, B. H., and R. J. O'Connell, Lithospheric thickening and subduction, plate motions and mantle convection, in *Physics of the Earth's Interior, Proc. Int. Sch. Phys. "Enrico Fermi"* edited by A. M. Dziewonski and E. Boschi, pp. 464–492, North Holland, Amsterdam, 1980.

Hart, S. R., A large-scale isotope anomaly in the Southern Hemisphere mantle, *Nature, 309*, 753–757, 1984.

Hart, S. R., Heterogeneous mantle domains: signatures, genesis and mixing chronologies, *Earth Planet. Sci. Lett., 90*, 273–296, 1988.

Hayes, D. E., Age-depth relationships and depth anomalies in the southeast Indian Ocean and south Atlantic Ocean, *J. Geophys. Res., 93*, 2937–2954, 1988.

Heestand, R. L., and S. T. Crough, The effect of hot spots on the oceanic age-depth relation, *J. Geophys. Res., 86*, 6107–6114, 1981.

Hetenyi, M., *Beams on Elastic Foundation*, The University of Michigan Press, Ann Arbor, 1974.

Jackson, E. D., and S. O. Schlanger, Regional syntheses, Line island chain, Tuamotu island chain, and Manihiki Plateau, Central Pacific Ocean, *Init. Repts. DSDP, 33*, 915–927, 1976.

Jarvis, G. T., and W. R. Peltier, Convection models and geophysical observations, in *Mantle Convection*, edited by W. R. Peltier, pp. 479–594, Gordon and Breach, New York, 1989.

Johnson, H. P., and R. L. Carlson, The variation of sea floor depth with age: a test of existing models based on drilling results, *Geophys. Res. Lett., 19*, 1971-1974, 1992.

Kaula, W. M., and R. J. Philips, Quantitative tests for plate tectonics on Venus, *Geophys. Res. Lett., 8*, 1187–1190, 1981.

Kirby, S. H., State of stress in the lithosphere: Inferences from the flow laws of olivine, *Pure and Applied Geophys., 115*, 245–258, 1977.

Kirby, S. H., Tectonic stresses in the lithosphere: Constraints provided by the experimental deformation of rocks, *J. Geophys. Res., 85*, 6353–6363, 1980.

Kirby, S. H., Rheology of the lithosphere, *Rev. Geophys. Space Phys., 21*, 1458–1487, 1983.

Langseth, M. G., X. Le Pichon, and M. Ewing, Crustal structure of the mid-ocean ridges, 5, Heat flow through the Atlantic Ocean floor and convection currents, *J. Geophys Res., 71*, 5321–5355, 1966.

Langseth, M. G., A. H. Lachenbruch, and B. V. Marshall, Geothermal observations in the Arctic region, in *The Geology of North America: The Arctic Ocean Region, L*, edited by A. Grantz, L. Johnson and J. F. Sweeney, pp. 188–152, GSA, Boulder, Colorado, 1990.

Larson, R. L., Latest pulse of Earth: Evidence for a mid-Cretaceous superplume, *Geology, 19*, 547–550, 1991.

Larson, R. L., and S. O. Schlanger, Cretaceous volcanism and Jurassic magnetic anomalies in the Nauru Basin, western Pacific Ocean, *Geology, 9*, 480–484, 1981.

Lister, C. R. B., On the thermal balance of a mid-ocean ridge, *Geophys. J. R. astron. Soc., 26*, 515–535, 1972.

Lister, C. R. B., J. G. Sclater, E. E. Davis, H. Villinger, and S. Nagihara, Heat flow maintained in oceanic basins of great age: investigations in the north-equatorial west Pacific, *Geophys. J. Int., 102*, 603–630, 1990.

Liu, M., and C. G. Chase, Evolution of midplate hot spot swells: numerical solutions, *J. Geophys. Res., 94*, 5571–5584, 1989.

Liu, M., and C. G. Chase, Boundary layer model of mantle plumes with thermal and chemical diffusion and buoyancy, *Geophys. J. Int., 104*, 433–440, 1991.

Louden, K. E., D. O. Wallace, and R. C. Courtney, Heat flow and depth versus age for the Mesozoic northwest Atlantic Ocean: results from the Sohm abyssal plain and implications for the Bermuda Rise, *Earth Planet. Sci. Lett., 83*, 109–122, 1987.

Louden, K. E., Marine heat flow data listing, Appendix B, in *Handbook of seafloor heat flow*, edited by J. A. Wright and K. E. Louden, pp. 325–485, CRC Press, Inc., Boca Raton, Florida, 1989.

Ludwig, W. J., and R. E. Houtz, *Isopach map of sediments in the Pacific Ocean Basin and Margina Sea Basins*, American Association of Petroleum Geologists, 1979.

Marty, J. C., A. Cazenave, and B. Lago, Geoid anomalies across Pacific fracture zones, *GJ, 93*, 1–23, 1988.

Marty, J. C., and A. Cazenave, Regional variations in subsidence rate of oceanic plates: a global analysis, *Earth Planet. Sci. Lett., 94*, 301–315, 1989.

McAdoo, D. C., and D. T. Sandwell, Folding of oceanic lithosphere, *J. Geophys. Res., 90*, 8563–8569, 1985.

McKenzie, D. P., Some remarks on heat flow and gravity anomalies, *J. Geophys. Res., 72*, 6261–6273, 1967.

McKenzie, D. P., and M. J. Bickle, The volume and composition of melt generated by extension of the lithosphere, *J. Petrol., 29*, 625–679, 1988.

McNutt, M. K., and H. W. Menard, Lithospheric flexure and uplifted atolls, *J. Geophys. Res., 83*, 1206–1212, 1978.

McNutt, M. K., Temperature beneath midplate swells: the inverse problem, in *Seamounts, Islands, and Atolls, Geophysical Monograph #43* edited by B. H. Keating, P. Fryer, R. Batiza and G. W. Boehlert, pp. 123–132, American Geophysical Union, Washington, D.C., 1987.

McNutt, M. K., and K. M. Fisher, The South Pacific Superswell, in *Seamounts, Islands, and Atolls, Geophysical Monograph #43* edited by B.H. Keating, P. Fryer, R. Batiza and G. W. Boehlert, pp. 25–34, American Geophysical Union, Washington, D.C., 1987.

McNutt, M. K., and A. V. Judge, The superswell and mantle dynamics beneath the South Pacific, *Science, 248*, 969–975, 1990.

McNutt, M. K., E. L. Winterer, W. W. Sager, J. H. Natland, and G. Ito, The Darwin Rise: A Cretaceous Superswell?, *Geophys. Res. Lett., 17*, 1101–1104, 1990.

McNutt, M., D. Caress, J. Mutter, and R. Detrick, Thickness of the elastic plate beneath the Marquesas islands: why is it so much greater than values elsewhere in French Polynesia?, *Eos Trans. AGU, 72 (supplement)*, 437, 1991.

Menard, H. W., *Marine Geology of the Pacific*, McGraw-Hill, New York, 1964.

Menard, H. W., Darwin reprise, *J. Geophys. Res., 89*, 9960–9968, 1984.

Menard, H. W., and M. McNutt, Evidence for and consequences of thermal rejuvenation, *J. Geophys. Res., 87*, 8570–8580, 1982.

Morgan, W. J., Deep mantle convection plumes and plate motions, *Am. Assoc. Petrol. Geol. Bull., 56*, 203–213, 1972.

Natland, J. H., and E. Wright, Magmatic lineages and mantle sources of Cretaceous seamounts in the Central Pacific, *Eos Trans. AGU, 65*, 1075–1076, 1984.

Nishimura, C. E., and D. W. Forsyth, Anomalous Love-wave phase velocities in the Pacific: sequential pure-path and spherical harmonic inversion, *Geophys. J. R. astron. Soc., 81*, 389–407, 1985.

Parmentier, E. M., and W. F. Haxby, Thermal stresses in the oceanic lithosphere: evidence from geoid anomalies at fracture zones, *J. Geophys. Res., 91*, 7193–7204, 1986.

Parsons, B., and J. G. Sclater, An analysis of the variation of ocean floor bathymetry and heat flow with age, *J. Geophys. Res.*, *82*, 803–827, 1977.

Parsons, B., and D. P. McKenzie, Mantle convection and the thermal structure of the plates, *J. Geophys. Res.*, *83*, 4485–4496, 1978.

Parsons, B., and F. M. Richter, Mantle convection and the oceanic lithosphere, in *Oceanic Lithosphere, (The Sea, vol. 7)*, edited by C. Emiliani, pp. 73–117, Wiley-Interscience, New York, 1981.

Parsons, B., and S. Daly, The relationship between surface topography, gravity anomalies, and temperature structure of convection, *J. Geophys. Res.*, *88*, 1129–1144, 1983.

Renkin, M. L., and J. G. Sclater, Depth and age in the North Pacific, *J. Geophys. Res.*, *93*, 2919–2935, 1988.

Robinson, E. M., B. Parsons, and M. Driscoll, The effect of a shallow low-viscosity zone on the mantle flow, the geoid anomalies and geoid and depth-age relationships at fracture zones, *Geophys. J.*, *93*, 25–43, 1988.

Robinson, E. M., and B. Parsons, Effect of a shallow low-viscosity zone on the formation of midplate swells, *J. Geophys. Res.*, *93*, 3144–3156, 1988.

Sandwell, D. T., and G. Schubert, Geoid height-age relation from SEASAT altimeter profiles across the Mendocino fracture zone, *J. Geophys. Res.*, *87*, 3949–3958, 1982.

Sato, H., I. S. Sacks, and T. Murase, Use of laboratory velocity data for estimating temperature and partial melt fraction in the low velocity zone: comparison with heat flow and electrical conductivity studies, *J. Geophys. Res.*, *94*, 5689–5704, 1989.

Schlanger, S. O., H. C. Jenkyns, and I. Premoli-Silva, Volcanism and vertical tectonics in the Pacific Basin related to global Cretaceous transgressions, *Earth Planet. Sci. Lett.*, *52*, 435–449, 1981.

Schlanger, S. O., and I. Premoli-Silva, Tectonic, volcanic, and paleogeographic implications of redeposited reef faunas of Late Cretaceous and Tertiary age from the Nauru Basin and the Line Islands, *Initial Rep. Deep Sea Drill. Proj.*, *61*, 817–828, 1981.

Schubert, G., C. Froidevaux, and D. A. Yuen, Oceanic lithosphere and asthenosphere: Thermal and mechanical structure, *J. Geophys. Res.*, *81*, 3525–3540, 1976.

Sclater, J. G., and L. Wixon, The relation between depth and age and heat flow and age in the western North Atlantic, in *The Geology of North America: The Western North Atlantic Region, M*, edited by P. R. Vogt and B. E. Tucholke, pp. 257–270, The Geological Society of America, 1986.

Sleep, N. H., Hot spots and mantle plumes: some phenomenology, *J. Geophys. Res.*, *95*, 6715–6736, 1990.

Sleep, N. H., Hot spots and mantle plumes, *Ann. Rev. Earth Planet. Sci.*, *20*, 19–43, 1992.

Sleep, N. H., and B. F. Windley, Archean plate tectonics: constraints and inferences, *J. Geol.*, *90*, 363–379, 1982.

Smith, W. H. F., H. Staudigel, A. B. Watts, and M. S. Pringle, The Magellan Seamounts: Early Cretaceous record of the South Pacific isotopic and thermal anomaly, *J. Geophys. Res.*, *94*, 10,501–10,523, 1989.

Smith, W. H. F., Marine geophysical studies of seamounts in the Pacific ocean basin, Ph.D. dissertation, Columbia University, New York, 1990.

Stein, C., and D. Abbott, Heat flow constraints on the South Pacific Superswell, *J. Geophys. Res.*, *96*, 16,083–16,100, 1991.

Stein, C. A., S. A. P. L. Cloetingh, and M. J. R. Wortel, Seasat-derived gravity constraints on stress and deformation in the northeastern Indian Ocean, *Geophys. Res. Lett.*, *16*, 823–826, 1989.

Stein, C. A., and S. Stein, A model for the global variation in oceanic depth and heat flow with lithospheric age, *Nature*, *359*, 123–129, 1992.

Stein, S., S. Cloetingh, D. Wiens, and R. Wortel, Why does near-ridge extensional seismicity occur preferentially in the Indian Ocean?, *Earth Planet. Sci. Lett.*, *82*, 107–113, 1987.

Stein, S., and E. A. Okal, Seismicity and tectonics of the Ninetyeast Ridge area: Evidence for internal deformation of the Indian plate, *J. Geophys. Res.*, *83*, 2233–2245, 1978.

Tracy, R. J., Petrology and genetic significance of an ultramafic xenolith suite from Tahiti, *Earth Planet. Sci. Lett.*, *48*, 80–96, 1980.

Turcotte, D. L., Properties of the lithosphere and asthenosphere deduced from geoid observations, in *Space Geodesy and Geodynamics*, edited by A. J. Anderson and A. Cazenave, pp. 451–475, 1986.

van der Hilst, R. D., and W. Spakman, Importance of the reference model in linearized tomography and images of subduction below the Caribbean plate, *Geophys. Res. Lett.*, *16*, 1093–1096, 1989.

Vogt, P. R., On the applicability of thermal conduction models to midplate volcanism: comments on a paper by Gass et al., *J. Geophys. Res.*, *86*, 950–960, 1981.

Von Herzen, R. P., R. S. Detrick, S. T. Crough, D. Epp, and U. Fehn, Thermal origin of the Hawaiian swell: Heat flow evidence and thermal models, *J. Geophys. Res.*, *87*, 6711–6723, 1982.

Von Herzen, R. P., M. J. Cordery, R. S. Detrick, and C. Fang, Heat flow and the thermal origin of hot spot swells: the Hawaiian swell revisited, *J. Geophys. Res.*, *94*, 13,783–13,799, 1989.

Watts, A. B., J. H. Bodine, and M. S. Steckler, Observations of flexure and the state of stress in the oceanic lithosphere, *J. Geophys. Res.*, *85*, 6369–6376, 1980.

Wessel, P., and W. Haxby, Thermal stress, differential subsidence, and flexure at oceanic fracture zones, *J. Geophys. Res.*, *95*, 375–391, 1990.

Wiens, D. A., and S. Stein, Age dependence of oceanic intraplate seismicity and implications for lithospheric evolution, *J. Geophys. Res.*, *88*, 6455–6468, 1983.

Winterer, E. L., Sedimentary facies and plate tectonics of the equatorial Pacific, *AAPG*, *57*, 265–282, 1973.

Winterer, E. L., Anomalies in the tectonic evolution of the Pacific, in *The Geophysics of the Pacific Ocean basin and its Margin, 19*, edited by G. H. Sutton et al., pp. 269–280, AGU, Washington, D. C., 1976.

Wolery, T. J., and N. H. Sleep, Hydrothermal circulation and geochemical flux at mid-ocean ridges, *J. Geol.*, *84*, 249–275, 1976.

Wolfe, C. J., and M. K. McNutt, Compensation of Cretaceous seamounts of the Darwin Rise, Northwest Pacific Ocean, *J. Geophys. Res.*, *96*, 2363–2374, 1991.

Woods, M. T., J.-J. Leveque, and E. A. Okal, Two-station measurements of Rayleigh wave group velocity along the Hawai'ian swell, *Geophys. Res. Lett.*, *18*, 105–108, 1991.

Wortel, M. J. R., M. J. N. Remkes, R. Govers, S. A. P. L. Cloetingh, and P. Th. Meijer, Dynamics of the lithosphere and the intraplate stress field, *Phil. Trans. R. Soc. Lond., Ser. A*, *337*, 111–126, 1991.

Wysession, M. E., E. A. Okal, and K. L. Miller, Intraplate seismicity of the Pacific basin, *Pure Appl. Geophys.*, *135*, 261–359, 1991.

Zhu, A., and D. A. Wiens, Thermoelastic stress in oceanic lithosphere due to hot spot reheating, *J. Geophys. Res.*, *96*, 18,323–18,334, 1991.

C. A. Stein, Department of Geological Sciences, University of Illinois at Chicago, Chicago, IL 60680.

S. Stein, Department of Geological Sciences, Northwestern University, Evanston, IL 60208.